Journal of chemical & engineering data

pubs.acs.org/jced

Article

Vapor–Liquid Equilibrium of Ionic Liquid 7-Methyl-1,5,7-triazabicyclo[4.4.0]dec-5-enium Acetate and Its Mixtures with Water

Zachariah Steven Baird, Petri Uusi-Kyyny,* Joanna Witos, Antti H. Rantamäki, Herbert Sixta, Susanne K. Wiedmer, and Ville Alopaeus

Cite This: *J. Chem. Eng. Data* 2020, 65, 2405–2421

Read Online

ACCESS | Metrics & More | Article Recommendations | Supporting Information

ABSTRACT: Ionic liquids have the potential to be used for extracting valuable chemicals from raw materials. These processes often involve water, and after extraction, the water or other chemicals must be removed from the ionic liquid, so it can be reused. To help in designing such processes, we present data on the vapor–liquid equilibrium of the system containing protic ionic liquid 7-methyl-1,5,7-triazabicyclo[4.4.0]dec-5-enium acetate, water, acetic acid, and 7-methyl-1,5,7-triazabicyclo[4.4.0]dec-5-ene. Earlier studies have only focused on mixtures of water and an ionic liquid with a stoichiometric ratio of the ions. Here, we also investigated mixtures containing an excess of the acid or base component because in real systems with protic ionic liquids, the amount of acid and base in the mixture can vary. We modeled the data using both the ePC-SAFT and NRTL models, and we compared the performance of different modeling strategies. We also experimentally determined the vapor composition for a few of the samples, but none of the modeling strategies tested could accurately predict the concentration of the acid and base components in the vapor phase.

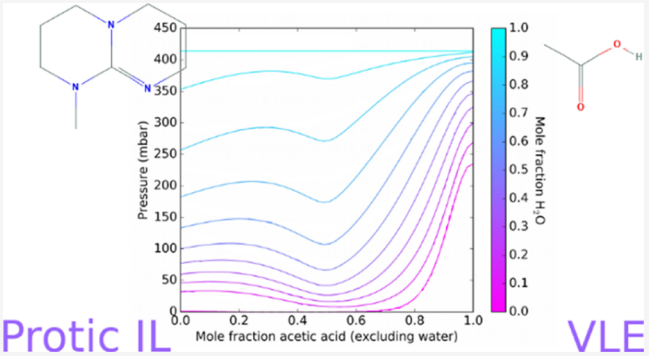

1. INTRODUCTION

Ionic liquids (ILs) are promising solvents for solid–liquid and liquid–liquid extraction.[1−4] For example, it has been found that 7-methyl-1,5,7-triazabicyclo[4.4.0]dec-5-enium acetate (mTBD acetate) can dissolve cellulose, and the Ioncell process uses this property to produce textile fibers from biomass.[2,5] Often these separation processes result in a solution of the IL and water (or another solvent), and the water must be removed before the IL can be recycled for subsequent extractions. Data on the vapor–liquid equilibrium (VLE) of such systems are necessary for modeling the evaporation processes commonly used to remove water.

Because of the importance of VLE data, many researchers have already made such measurements. NIST's database for ionic liquids (ILThermo)[6] currently contains more than 100 data sets for VLE measurements involving ILs and water, and there are more data that ILThermo has not captured.[7] However, most of this data is for aprotic ILs. In recent years, there has been increasing interest in protic ILs, which are often cheaper and easier to synthesize.[8] Protic ILs are formed via a proton transfer reaction between an acid and a base, and because of the equilibrium between the IL and the reactants, the composition of the IL can change during separation processes. To our knowledge, there have been no publications investigating how the vapor pressure of aqueous IL solutions changes when the ratio between acid and base components varies. One article by Ribeiro et al.[9] reports vapor pressures over a narrow range of compositions with an excess of acid, but it does so only for systems containing the acid and the base, no water.

In real processes, the ratio of the acid and base components often deviates from 1:1, especially because many protic ILs exhibit a reactive azeotrope (or possibly formation of a complex) at compositions other than an equimolar ratio.[9−12] An excess of one component may also be desirous if it results in improved properties for a particular use. For instance, Wijaya et al.[13] varied the ratio of acid to base to modify the acidity/basicity of their solutions, and Mazaheripour et al.[14] showed that they could tailor the Seebeck coefficient of films by adjusting the ratio of acid to base in the ionic liquid additive. For these reasons, one of our aims was to investigate how VLE behavior changes as the acid to base ratio deviates from 1:1.

Many of the common thermodynamic models have been used for modeling the VLE of ionic liquid systems, including

Received: October 30, 2019
Accepted: April 16, 2020
Published: April 28, 2020

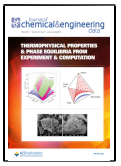

https://dx.doi.org/10.1021/acs.jced.9b01039
J. Chem. Eng. Data 2020, 65, 2405–2421

Table 1. Information About the Chemicals Used in This Work

chemical	InChI key		purification	water content (wt %)	purity	analysis method
water	XLYOFNOQVPJJNP-UHFFFAOYSA-N	In house	Millipore Elix 20		<1 μg/L of ionic compounds	electrical resistance
acetic acid	QTBSBXVTEAMEQO-UHFFFAOYSA-N	Sigma Aldrich	molecular sieves and distillation	0.013	99.9 wt %	GC[a]
acetic acid	QTBSBXVTEAMEQO-UHFFFAOYSA-N	Merck	none	0.11	99.5 wt %	GC
7-methyl-1,5,7-triazabicyclo[4.4.0]dec-5-ene	OEBXWWBYZJNKRK-UHFFFAOYSA-N	University of Helsinki	none	0.03	100.9 ± 1.4 wt %	CE[b]
7-methyl-1,5,7-triazabicyclo[4.4.0]dec-5-ene	OEBXWWBYZJNKRK-UHFFFAOYSA-N	BOC Sciences	vacuum distillation	0.01	98.3 ± 1.7 wt %	CE

[a]Gas chromatography. [b]Capillary electrophoresis.

the NRTL, Wilson, UNIQUAC, eNRTL, UNIFAC, COSMO-RS, ePC-SAFT, and SAFT models.[15−23] Often, the ionic liquid is simply modeled as a molecular species. However, some researchers have used more complicated electrolyte models such as eNRTL and ePC-SAFT.[24−27] We did not find any examples in the literature in which researchers modeled the VLE in a way that allowed the ratio between acid and base to change, and this was a second aim of our study. Models that work for varying compositions of acid and base are important for real industrial processes.

2. METHODS

2.1. Preparation of Chemicals. Information about the chemicals used in this study is summarized in Table 1. Water was purified on site with a Millipore Elix 20 purification system. The 7-methyl-1,5,7-triazabicyclo[4.4.0]dec-5-ene (mTBD) used for most of the experiments was synthesized and purified at the University of Helsinki. A second sample of mTBD was obtained from BOC Sciences (Shirley, NY, USA), and this was purified via vacuum distillation. The first sample was used for most of the experiments. The first sample of acetic acid was purchased from Sigma-Aldrich. It was dried using 3 Å molecular sieves. The acetic acid had a brownish tint after drying, so it was then distilled to get pure acetic acid. The second sample of acetic acid was purchased from Merck, and no additional purification was performed.

The water from the Millipore Elix 20 had a resistance of 18.2 MΩ cm at 298 K, which corresponds to a concentration of ionic compounds that is less than 1 μg/L. The water contents of the mTBD and acetic acid were measured using a DL38 Karl Fischer Titrator (Mettler Toledo, Columbus, OH, USA). The purity of the acetic acid was assessed using a gas chromatograph with a flame ionization detector. Because water does not give a signal with this detector, the water content from Karl Fischer titration was taken into account when calculating the purity. The purity of the mTBD was determined using a capillary electrophoresis method described in our earlier article.[28]

All VLE measurements where water was present were made with the first sample from the University of Helsinki. The second sample was used for mixtures that contained only acetic acid and mTBD.

2.2. Composition Analysis. Most of the samples were prepared gravimetrically, and therefore, the composition was known. For a few of the samples, the compositions were also measured using capillary electrophoresis. A description of this method for measuring mTBD concentrations was given in our earlier article.[28]

The concentration of the acetate was determined using a modified capillary zone electrophoresis method published elsewhere.[29] In short, the background electrolyte (BGE) was a buffer solution containing 20 mM 2,3-pyridinecarboxylic acid (Sigma-Aldrich, Steinheim, Germany) and 0.3 mM myristyltrimethylammonium hydroxide (100 mM concentrate, Waters, Milford, USA) in 10:90 (v/v) MeOH/H_2O. The pH of the solution was adjusted to 9 using 25% (v/v) ammonia. The buffer was filtered through a 0.45 μm PVDF filter (Aireka Cells, Wan Chai, Hong Kong) before use.

The capillary electrophoresis device used in the study was a Hewlett Packard 3D CE model G1600GX. The silica capillary length and the distance to the detector were 38.5 and 30 cm, respectively. The capillary was preconditioned before each run by flushing at 940 mbar for 1 min with 0.1 M NaOH, 1 min with ultrapure water, and 3 min with BGE, and finally a voltage of +20 kV was applied for 20 s. The sample was injected hydrodynamically at 45 mbar for 10 s. The separation was performed using a voltage of −10 kV, and the detection was done using a diode-array UV−vis detector at 254 nm.

For acetate quantification, nine acetic acid (Fluka/Sigma-Aldrich, Steinheim, Germany) solutions with concentrations between 0.0025 and 0.2 mg/mL were analyzed. In these calibration solutions and in the IL samples under investigation, propionic acid (Acros Organics/Thermo Fischer Scientific, Geel, Belgium) with a 0.05 mg/mL concentration was used as an internal standard. The correlation coefficient of the calibration curve was 0.9997.

2.3. Static Total Pressure Apparatus. Most of the VLE measurements were performed using a static total pressure apparatus, and this apparatus was also used for some of our earlier VLE measurements.[7] Each cell consisted of a metal cylinder at the bottom that held the sample, a pressure sensor at the top, and valves and fittings in between. A valve separated the lower part of the cell, which contained the sample, from the upper part, where the pressure sensor was located. A more complete description of the apparatus, including schematics of the cell, was given by Ostonen et al.[7] The volume of each cell can be found on the Open Science Framework project accompanying this article (https://osf.io/cbe3j/) or in Supporting Information. TERPS 8000 pressure sensors were used (GE, Boston, MA, USA), and the expanded uncertainty of these pressure sensors, as stated by the manufacturer, was between 1.4 and 3.5 mbar (depending on the range of the sensor). Temperatures were measured using an F200 temper-

https://dx.doi.org/10.1021/acs.jced.9b01039
J. Chem. Eng. Data 2020, 65, 2405−2421

ature meter (Tempcontrol, Nootdorp, Netherlands), which had been calibrated at the Finnish National Metrology Institute (Espoo, Finland). The expanded uncertainty of the temperature probe was 0.03 K ($k = 2$), as determined from the results of the calibration.

The mixtures were made directly in the lower part of each cell. The masses of the components added were measured using a Precisa 410AM-FR balance (Dietikon, Switzerland), which had a repeatability of 0.00085 g. The uncertainties for the compositions were calculated based on this repeatability, and these uncertainties are given in the data file (see https://osf.io/cbe3j/ or Supporting Information). On average, the expanded uncertainty (95% level) of the composition was 0.04 mol %. In total, about 10 g of the sample was added to each cell. The mTBD and acetic acid react when mixed, the released heat can cause water to evaporate. To avoid this, the cells were cooled in an ice bath and the acetic acid was added slowly. Additionally, the valve opening was covered to prevent any vapor from escaping.

After mixing, the samples were degassed. Liquid samples were degassed for at least 20 min in an ultrasonic bath. Some of the samples were solid at room temperature. To degas these samples, the air in the cell was first removed using a vacuum pump. Then, the cell was closed and placed in a bath at 358 K to melt the sample. The sample was then cooled and reconnected with the vacuum pump to remove any air that had been released. The solid samples were melted three times in this manner. Each cell was remeasured to determine how much of the sample was lost during degassing. The average weight loss of the aqueous mixtures was 1.5%. It was assumed that water was the only compound that evaporated, and measurements with the circulation still showed this to be a valid assumption. The compositions were slightly adjusted to account for this loss during degassing. For the mixtures without water, the degassing time was increased, leading to a larger mass loss. For these samples, the composition was measured at the end of the experiment by measuring the refractive index of the sample (see Section 2.4).

After degassing, the lower part of each cell was connected to its upper part. Then, the upper part was evacuated using a vacuum pump. The valve separating the lower and upper parts was kept closed to allow the upper part to be checked for leaks. After leak testing, the cells were placed in a rack in an oven and the valve separating the lower and upper parts was opened. An RTD thermometer was placed in the middle of the rack between the 4 cells. The rack was continuously rocked to keep the samples in the cells well mixed. Once all 4 cells were in place, the oven was heated to the desired temperatures. Values were recorded once the pressure and temperature readings had stabilized, which took about 1 to 2 h. Measurements were made between 303 and 353 K.

mTBD can hydrolyze; so to check that hydrolysis did not affect the results, a repeat measurement was performed at the end of the run at the same temperature as the first point. This also verified that no significant leak had occurred during the run. No deviation was noticed between these repeat measurements, so any possible hydrolysis can be neglected for these experimental conditions. For four of the mixtures, we also reanalyzed the contents of the cell after the measurement was complete. No hydrolysis products were detected in any of these four samples.

To check the uncertainty of the apparatus, the vapor pressure of water was measured. The results were compared to reference values for water from the IAPWS95 equation of state.[30] Based on these results, the standard uncertainty of the apparatus was calculated to be 2.3 mbar (expanded uncertainty of 5.6 mbar at the 95% level). The average relative deviation of the measured values was 1.4%.

2.4. Circulation Still Experiment. To investigate the extent to which ionic liquid components transfer to the vapor phase, a set of experiments was conducted in a circulation still. The circulation still was built by the glass workshop at Aalto University, based on the design presented by Yerazunis et al.,[31] with some modifications. The heart of the device is the equilibrium chamber, which is where VLE is achieved. Following the equilibrium chamber, the vapor and liquid phases are separated, and the vapor phase is condensed. There are two small chambers where the vapor and liquid phases are collected, which allows samples of both phases to be taken. From these collection chambers, the fluids then flow back to a reboiler where the mixture is vaporized and flows back to the equilibrium chamber. More details about the circulation still can be found in our earlier articles.[32,33]

The temperature in the equilibrium chamber was measured using a Pt-100 resistance thermometer that was connected to an F200 temperature meter (Tempcontrol, Nootdorp, Netherlands). The expanded uncertainty of the temperature measurement was estimated to be 0.12 K, when taking into account temperature fluctuations during the experiment. The pressure in the still was measured using a Druck PMP 4070 pressure transducer (Baker Hughes, Houston, TX, USA), which was calibrated with a Beamex MC2-PE pressure calibrator (Pietarsaari, Finland). Based on this calibration, the standard uncertainty of the pressure sensor was calculated to be 0.33 mbar (expanded uncertainty of 0.76 mbar at the 95% level).

The apparatus was tested by measuring the vapor pressure of purified water. This data can be found in the data file (see https://osf.io/cbe3j/ or Supporting Information). The experimental values were compared to reference values from the IAPWS95 equation of state.[30] The results showed good agreement with the reference values, with a maximum deviation of only 0.37 kPa. Based on these experimental results, the standard uncertainty of the setup was calculated to be 0.18 kPa (expanded uncertainty of 0.38 kPa at the 95% level).

One advantage of the circulation still is that it allows the vapor and liquid phases to be sampled and analyzed. For the aqueous solutions, the concentration of mTBD in these samples was analyzed using the same capillary electrophoresis method described in our earlier article,[28] and the concentration of acetic acid was determined using the capillary electrophoresis method described in Section 2.2. The water content of the samples was calculated by difference using the results for mTBD and acetic acid. To check these values, the water content was also measured using gas chromatography with a thermal conductivity detector. The gas chromatograph was calibrated using gravimetrically prepared samples. These measured concentrations matched with those calculated from the capillary electrophoresis data to within the uncertainty of the gas chromatographic method. However, because the uncertainty of the values calculated by difference from the capillary electrophoresis data was smaller, these values are reported.

Measurements were also made with only acetic acid and mTBD in the still. The data for these measurements showed a larger positive deviation from the literature value of the vapor

https://dx.doi.org/10.1021/acs.jced.9b01039
J. Chem. Eng. Data 2020, 65, 2405−2421

pressure of pure acetic acid. Although no water was added for these measurements, it is still likely that a small amount of water was present as a light impurity. As a result, the expanded uncertainty for these measurements is estimated to be larger, about 2 kPa.

For these measurements, the composition was determined by measuring the refractive index of the samples taken from the device. A calibration curve for converting between refractive index and mTBD concentration was created using mixtures of mTBD and acetic acid that had been prepared gravimetrically. This data are given in Table 2, and the calibration curve was a second order polynomial fit to the data. Based on the calibration, the standard uncertainty of the mole fraction was estimated to be 0.0015 (expanded uncertainty of 0.0035 at the 95% level).

Table 2. Experimental Values of the Refractive Index for Mixtures of Acetic Acid and mTBD Measured at 1000 mbar

refractive index nD at 293.15 K[a]	mole fraction of mTBD	mole fraction of acetic acid	standard uncertainty of mole fraction[b]	expanded uncertainty of mole fraction (95% level)
1.3716	0.0000	1.0000		
1.3853	0.0196	0.9804	0.00018	0.00040
1.3904	0.0278	0.9722	0.00020	0.00044
1.4289	0.1048	0.8952	0.00032	0.00070
1.4476	0.1535	0.8465	0.00035	0.00078
1.4164	0.0764	0.9236	0.00032	0.00070
1.4031	0.0504	0.9496	0.00005	0.00011
1.4266	0.0996	0.9004	0.00005	0.00012
1.4460	0.1492	0.8508	0.00006	0.00013
1.4631	0.1905	0.8095	0.00006	0.00014

[a]Standard uncertainty of the refractive index at 1000 mbar is 0.00034 (expanded uncertainty of 0.00078 at 95% level). The expanded uncertainty of the temperature is 0.03 K. [b]Calculated based on the standard uncertainty of the balance, which was 0.00085 g.

3. MODELING

3.1. Modeling Using ePC-SAFT. ePC-SAFT was one of the two models used for modeling the VLE behavior of the mTBD acetate + water system. The ePC-SAFT model adds an electrolyte term to the PC-SAFT equation of state and was originally proposed by Cameretti et al.[34,35] Later, Held et al.[18] published an improved version of the ePC-SAFT model in which dispersion interactions between anions and cations are included, and we used this version of ePC-SAFT. Because acetic acid and water are associating compounds, we also included the PC-SAFT term for association interactions.[36−40] Our code implementing ePC-SAFT can be found on GitHub (https://github.com/zmeri/PC-SAFT).

One parameter in the electrolyte term of ePC-SAFT is the dielectric constant of the solution. For aqueous electrolyte systems, the dielectric constant is usually kept equal to that of water and the effect of dissolved ions is not considered.[34] We have used this approach for systems based on literature data (those for which $mTBDH^+$ is not present), but for mixtures containing the ionic liquid, the dielectric constant was calculated as the weighted average of the dielectric constant of each component. Weights were based on the mole fraction of each component. The dielectric constant of water was modeled by fitting polynomial equations to data reported from Archer and Wang.[41] One equation was used at temperatures up to 368.15 K (eq 1), and above that temperature, the second polynomial was used (eq 2). This allowed the dielectric constant to be calculated at temperatures above the boiling point of water.

$$\epsilon_{water} = 7.6555618295\cdot10^{-04}\cdot T^2 - 0.81783881423\cdot T + 254.19616803 \quad (1)$$

$$\epsilon_{water} = 0.0005003272124\cdot T^2 - 0.6285556029\cdot T + 220.4467027 \quad (2)$$

In eqs 1 and 2, T is the temperature (K). The dielectric constant for acetic acid (value of 6.15) was obtained from the DIPPR database.[42] No data could be found on the dielectric constants of mTBD or mTBD acetate. For mTBD, a value of 2.5 was used because this is the value for 1-methyltetralin, which also has two rings and a methyl group.[42] Also, for mTBD acetate, a value of 25 was used based on data for other protic ionic liquids reported by Weingärtner.[43]

We included five components in the model for the aqueous mTBD acetate system: water, acetic acid, mTBD, the ions $mTBDH^+$, and acetate. In reality, mTBD also reacts with water, so the hydroxide ion is also present; however, including the hydroxide ion in the model gave poor results. This is likely because including it gave the model too many parameters, and in areas between experimental data points, large jumps in calculated properties were observed (see discussion in Section 4.3). The reaction between mTBD and acetic acid was modeled using eq 3, the van't Hoff equation.[44,45]

$$K = \exp\left(\frac{\Delta H_{rxn}}{R}\cdot\left(\frac{1}{T} - \frac{1}{T_0}\right)\right)\cdot K_0 \quad (3)$$

In eq 3, K is the equilibrium constant of the reaction, K_0 is the equilibrium constant at the reference temperature T_0 (we used 298 K), ΔH_{rxn} is the enthalpy of the reaction at the reference temperature (J mol^{-1}), R is the ideal gas constant (J mol^{-1} K^{-1}), and T is the temperature (K). We did not have experimental data on the equilibrium of the ionic liquid reaction, so we chose the enthalpy of reaction to be −70,000 J mol^{-1} based on the value for 1,5-diazabicyclo(4.3.0)non-5-enium acetate, which is structurally similar to mTBD.[46,47] We set K_0 to be 10,000 because mTBD is a strong base, and we expect it to react almost completely with acetic acid.[48]

We also accounted for association interactions between water and the hydroxide and acetate ions.[49] Association interactions between ions have also been shown to be important for protic ionic liquids.[50,51] Association was taken into account by including the association volume (κ^{AB}) for the ions as one of the parameters to be fit. The association energy (ε^{AB}) was set to zero. This method has been used before by Held et al.[52] for modeling solutions containing methyldiethanolamine. At first, we also included the association volume parameter for $mTBDH^+$, but after an initial optimization it was left out because the value became quite small and did not have a noticeable effect on the accuracy.

The model also involved two different interaction parameters: k_{ij} and l_{ij}. In some cases, a temperature dependent k_{ij} was used, as defined in eq 4.[18]

$$k_{ij} = k_{base} + k_T\cdot T \quad (4)$$

In eq 4, k_{base} and k_T are parameters fit for a specific binary pair and T is the temperature (K).

https://dx.doi.org/10.1021/acs.jced.9b01039
J. Chem. Eng. Data 2020, 65, 2405−2421

Table 3. PC-SAFT Parameters for the Compounds Used in This Study[b]

component	m	Σ	ε/k	κ^{AB}	ε^{AB}/k	z	reference
H_2O	1.2047	[a]	353.95	0.0451	2425.67	0	129
mTBD	4.1308	3.6822	323.47			0	28
$mTBDH^+$	5.8352	3.3716	419.82			1	
HAc	1.3403	3.8582	211.59	0.075550	3044.4	0	36
Ac^-	1.4886	3.5345	294.53	0.018209	0	−1	
Li^+	1	2.3964	379.12			1	
Na^+	1	2.8935	167.14			1	
K^+	1	1.7374	238.06			1	
Cl^-	1	2.9696	292.88			−1	
Br^-	1	3.0976	373.41			−1	
I^-	1	3.1723	363.24			−1	

[a]A temperature dependent σ was used for water (given by eq 5). [b]Sec m is the segment number, σ is the segment diameter (Å), ε/k is the dispersion energy divided by the Boltzmann constant (K), κ^{AB} is the association volume, ε^{AB}/k is the association energy divided by the Boltzmann constant (K), z is the charge of the component, and Ac^- is the acetate ion.

The PC-SAFT parameters for water, acetic acid, and mTBD were available in the literature.[18,28,36] We did, however, make a slight modification for water. To be able to accurately calculate the density of water using PC-SAFT, the segment diameter (σ) is usually defined to be a function of temperature. This approach was introduced by Cameretti and Sadowski,[53] and we have used the same equation form as them. However, we refit the constants of the equation to extend the temperature range up to 473 K. This was done by solving for σ at each of 40 different temperatures between 273.16 and 473.15 K using reference density values from the IAPWS95 equation of state.[30] Then, the equation form given by Cameretti and Sadowski was fit to the σ values. The resulting equation is given as eq 5

$$\sigma = 3.8395 + 1.2828 \cdot e^{(-0.0074944 \cdot T)} - 1.3939 \cdot e^{(-0.00056029 \cdot T)} \quad (5)$$

where T is the temperature (K). This equation is valid for temperatures between 273.16 and 473.15 K. At temperatures up to 373 K, the densities and vapor pressures calculated using eq 5 are very similar to those calculated using the constants reported from Cameretti and Sadowski. However, above 373 K, eq 5 provides more accurate results. Overall, the average relative deviation of the PC-SAFT model when using eq 5 is 0.02% for density and 0.9% for vapor pressure.

We optimized the PC-SAFT parameters for $mTBDH^+$, the acetate ion, and binary interactions by using experimental VLE and density data. The VLE data are given in Table 7. The density data will be presented in a separate article about the properties of this system. Both the VLE and density data are also available in an Open Science Framework project accompanying this article (https://osf.io/krx5z/) or in Supporting Information. One important side note about the data is how molar densities were calculated. Molar densities are calculated using eq 6

$$\rho = \frac{\rho_{mass} \cdot 1000}{\sum_i x_i \cdot M_i} \quad (6)$$

where ρ is the molar density (mol m^{-3}), ρ_{mass} is the mass based density (kg m^{-3}), x_i is the mole fraction of component i in the mixture, and M_i is its molar mass. For electrolyte PC-SAFT, the ions are considered to be separate components in the solution (i.e., that they are dissociated), so when calculating molar densities each ion appears separately in the denominator. In contrast, elsewhere in the literature, the cation−anion pair is often counted as a single species, at least for the purpose of molar calculations.[54] This difference affects the total number of moles calculated for the system as well as the molar density, and it should be noted when comparing molar densities calculated by electrolyte PC-SAFT to those given elsewhere.

Although parameters for the acetate ion were given earlier by Held et al.,[18] these parameters were only fit to data at 298.15 K. Therefore, we refit the parameters using the procedure outlined by Held et al.[18] in which they first fit parameters for alkali cations and halide anions and then successively fit the parameters for the remaining ions. This procedure also fit the interaction parameters between the ions and water and between the cations and anions. Literature data were used to fit these parameters, as well as to fit the interaction parameter between water and acetic acid, and files containing this literature data can be found from the OSF project accompanying this article (https://osf.io/prx48/).[55−126] Optimization was performed using the differential evolution solver implemented in the SciPy package for Python.[127,128] All the PC-SAFT parameters used or fit in this study are given in Table 3.

The pure component parameters for $mTBDH^+$ and all remaining interaction parameters were optimized using experimental data we measured. First, the interaction parameters between mTBD and water were optimized using binary VLE and density data. Then, the remaining interaction parameters and the parameters for $mTBDH^+$ were optimized using the rest of the VLE and density data. The VLE data used for determining these PC-SAFT parameters is given in Table 7, and both the VLE and density data can also be obtained from the OSF project accompanying the article (https://osf.io/prx48/).

Optimization was performed by minimizing the objective function using the differential optimization solver implemented in the Scipy package for Python.[127,128] Both density and VLE data were used in optimization, but the vapor pressure was not directly calculated. Calculating the pressure for the VLE data would require another internal solver loop, which slowed down the overall optimization. Instead, the value from the function used to solve for the VLE pressure was minimized directly, as presented in eq 8. We tested and found that when the square root of this value was multiplied by 100 the resulting value closely matched the percent error of the vapor pressure. The objective function is given in eqs 7 and 8

https://dx.doi.org/10.1021/acs.jced.9b01039
J. Chem. Eng. Data 2020, 65, 2405−2421

Table 4. PC-SAFT Interaction Parameters Optimized and Used in This Study[a]

type of parameter	i	J	value	type of parameter	i	j	value
k_{ij}	Li^+	Ac^-	−0.878	k_{ij} (k_T)	H_2O	$mTBDH^+$	-9.497×10^{-3}
k_{ij}	Li^+	Cl^-	0.765	l_{ij}	H_2O	$mTBDH^+$	0.609
k_{ij}	Li^+	Br^-	0.667	k_{ij}	H_2O	Li^+	−0.213
k_{ij}	Li^+	I^-	0.517	k_{ij} (k_{base})	H_2O	Na^+	1.0128
k_{ij}	Na^+	Ac^-	0.014	k_{ij} (k_T)	H_2O	Na^+	-2.5333×10^{-3}
k_{ij}	Na^+	Cl^-	−0.280	k_{ij} (k_{base})	H_2O	K^+	1.7625
k_{ij}	Na^+	Br^-	0.186	k_{ij} (k_T)	H_2O	K^+	-3.1543×10^{-3}
k_{ij}	Na^+	I^-	0.713	k_{ij}	H_2O	Cl^-	−0.463
k_{ij}	K^+	Ac^-	0.756	k_{ij}	H_2O	Br^-	−0.238
k_{ij}	K^+	Cl^-	−0.259	k_{ij}	H_2O	I^-	−0.103
k_{ij}	K^+	Br^-	−0.161	k_{ij}	mTBD	$mTBDH^+$	0.277
k_{ij}	K^+	I^-	0.499	k_{ij}	mTBD	HAc	−1.588
k_{ij}	H_2O	HAc	−0.127	k_{ij}	mTBD	Ac^-	−0.141
k_{ij}	H_2O	Ac^-	0.007	k_{ij}	$mTBDH^+$	HAc	0.322
k_{ij} (k_{base})	H_2O	mTBD	−6.3649	k_{ij} (k_{base})	$mTBDH^+$	Ac^-	−0.405
k_{ij} (k_T)	H_2O	mTBD	3.0774×10^{-4}	k_{ij} (k_T)	$mTBDH^+$	Ac^-	3.4323×10^{-4}
l_{ij}	H_2O	mTBD	0.48316	l_{ij}	$mTBDH^+$	Ac^-	0.076
k_{ij} (k_{base})	H_2O	$mTBDH^+$	−5.420	k_{ij}	HAc	Ac^-	0.076
k_{ij} (k_T)	H_2O	mTBD	3.0774×10^{-4}	k_{ij}	HAc	Ac^-	−1.497

[a] Ac^- is the acetate ion.

$$\sum_n \frac{(\rho_{calc} - \rho_{exp})}{\rho_{exp}} \cdot 100 + \theta_{VLE} \tag{7}$$

$$\theta_{VLE} = \left(\begin{array}{l} \left(\sum_n \left(V - \frac{\beta n}{\rho_v} - \frac{(1-\beta)n}{\rho_l} \right)^2 \right. \\ \left. + \sum_j (x_{l,j}\phi_{l,j} - x_{v,j}\phi_{v,j})^2 \right. \\ \left. + \sum_i (n x_{tot,i} - \beta n x_{v,i} - (1-\beta) n x_{l,i})^2 \right)^{0.5} \end{array} \right) \cdot 100 \tag{8}$$

where ρ_{calc} is the molar density calculated with PC-SAFT (mol m^{-3}); ρ_{exp} is the experimental molar density (mol m^{-3}); V is the volume of the cell in the static total pressure apparatus (m^3); β is the overall fraction of the mixture in the vapor phase in terms of moles; n is the total number of moles in the cell; ρ_v is the density of the vapor phase (mol m^{-3}); ρ_l is the density of the liquid phase (mol m^{-3}); j is the index for the molecular species; i is the index for all components (including the ions); n is the index for each data point; x is the mole fraction of each component in the liquid phase (l), vapor phase (v), or whole cell (tot); and Φ is the fugacity coefficient of each component in the liquid or vapor phase. Most of the VLE data was PTz data, where only the total composition was known. For the bubble point VLE data, only the middle term in eq 8 was used.

The interaction parameters optimized in this study are presented in Table 4.

Also note that with ePC-SAFT, and with almost any other model, ionic components are considered nonvolatile.[18,34] This means that the models do not allow the ionic components to be present in the vapor phase. This simplification is generally accepted, even though some ionic compounds do appear in the vapor phase, because the concentration of ions is quite small, as has been shown for NaCl.[130] We also confirmed the validity of this assumption experimentally by measuring the vapor phase composition for a couple points in the circulation still apparatus (see Section 4.2).

3.2. Modeling Using NRTL. An NRTL model was developed to model the mTBD acetate + water system. To be able to describe the behavior, an additional component was included that corresponded to a hypothetical complex formed between the ionic liquid and acetic acid. This additional IL component was specified as containing 3 molecules of acetic acid and 2 of mTBD. This ratio was chosen, instead of 1 molecule of acid and 1 of mTBD, because protic ionic liquids have been shown to have a minimum in the pressure at composition with more than 1 acid molecule for each base molecule.[9,11] This method was used earlier by Ahmad et al.[11] Water, acetic acid, and mTBD were also included as components in the model. The amount of the 3:2 IL component in the system was calculated using the simple assumption that the mTBD and acetic acid reacted to completion, so free mTBD and acetic acid were not present at the same time. For the vapor phase, the ideal gas law was used.

In the NRTL model, the binary parameters τ_{ij} and τ_{ji} and the nonrandomness factor α must be specified for each pair of components.[15] Note that the τ parameters are nonsymmetric, so τ_{ij} is usually not equal to τ_{ji}. α was kept at 0.3 for all pairs. τ_{ij} and τ_{ji} are temperature dependent parameters, and we used a simple two parameter equation for this temperature dependence, which is shown in eq 9.

$$\tau_{ij} = \tau_{base} + \frac{\tau_T}{T} \tag{9}$$

In eq 9, T is the temperature (K) and τ_{base} and τ_T are parameters specific to each binary pair. The Python code we wrote for implementing the NRTL model can be found on GitHub (https://github.com/zmeri/NRTL).

https://dx.doi.org/10.1021/acs.jced.9b01039
J. Chem. Eng. Data 2020, 65, 2405−2421

τ_{ij} and τ_{ji} for the acetic acid + water pair were fit to literature data.[97−99,101−126] τ_{ij} and τ_{ji} for mTBD and water were fit to binary VLE data we measured, as were τ_{ij} and τ_{ji} for acetic acid and the 3:2 IL component. Because mTBD and acetic acid are never present at the same time when using the reaction scheme we used, the parameters for this pair were kept at 0. Additionally, no interaction parameter was used between the mTBD and IL because no binary data was available and because including the parameter led to jumps in the pressure at some compositions. For the acetic acid + IL pair, τ_{ij} and τ_{ji} were specified to be independent of temperature (τ_T was set to 0). The parameters for the IL + water pair were optimized using the remaining VLE data. For optimizing the NRTL parameters, we used the differential evolution solver that is included in the Scipy package for Python.[127,128] The parameters we obtained are given in Tables 5 and 6.

Table 5. Temperature Independent Parameter for the NRTL Equation (τ_{base})

		I			
		water	Acetic acid	mTBD	3:2 IL component
J	Water	0	20.656	−1.21966	27.9998
	acetic acid	0.55677	0	0	13.574
	mTBD	0.352130	0	0	0
	3:2 IL component	−3.35329	−6.8420	0	0

Table 6. Temperature Dependent Parameter for the NRTL Equation (τ_T)

		i			
		water	acetic acid	mTBD	3:2 IL component
J	Water	0	5967.62	978.478	−4226.30
	acetic acid	−51.6547	0	0	0
	mTBD	−857.380	0	0	0
	3:2 IL component	−863.692	0	0	0

To calculate vapor liquid equilibria using the NRTL model, the vapor pressures of the pure components must also be given. For water, the IAPWS95 equation of state was used, which is implemented in the CoolProp library.[30,131] For acetic acid, the DIPPR correlation was used (see the dippr_acid function in our Python code at https://github.com/zmeri/NRTL). For mTBD, the PC-SAFT equation of state was used (code available at https://github.com/zmeri/PC-SAFT), and the parameters were taken from our earlier article (see also Table 3).[28] For the 3:2 IL component, we fit the Antoine equation to experimental vapor pressure data for the IL at this composition (experimental data available at https://osf.io/cbe3j/ or in Supporting Information). The Antoine equation is shown as eq 10

$$\ln P = 21.51562 - \frac{3431.730}{T - 200} \tag{10}$$

where P is the vapor pressure (Pa) and T is the temperature (K).

4. RESULTS AND DISCUSSION

4.1. Effect of Temperature and Composition on Pressure. VLE data were measured for 28 different compositions at temperatures between 303 and 353 K using a static total pressure apparatus. These data are given in Table 7 and has also been placed in a scientific repository (Open Science Framework). Additional information about the data, including the uncertainties of the compositions, can be found in the data file at the Open Science Framework (https://osf.io/cbe3j/) or in the Supporting Information.

To model the VLE data, we compared two different models: the electrolyte PC-SAFT (ePC-SAFT) equation of state and the non-random two liquid (NRTL) activity coefficient model.[15,18,34] Details about the way we implemented these models are in Sections 3.1 and 3.2. The ePC-SAFT model had a root mean squared relative error of 16%, and for the NRTL model, it was 24%. The relative deviation for each data point is shown in Figure 1.

The models can be used to show how the vapor pressure of the system changes depending on the temperature and liquid composition (Figure 2) and can also highlight some of the interesting behavior of this system. When plotted in terms of mole fraction, it can be seen that the system exhibits a negative deviation from Raoult's law, which has been observed before for other aqueous systems with similar ionic liquids.[9,11] When viewed in terms of mole fraction, it would appear that the vapor pressure decreases rapidly as more mTBD acetate is added. However, when viewed in terms of mass fraction the largest decreases in the vapor pressure only really occur when mTBD acetate makes up more than 50 wt % of the solution.

It is also helpful to look at simpler systems, such as binary systems, to verify that the models give correct behavior when some of the components are not present. For the mTBD + water system, the vapor pressure is shown in Figure 3. The acetic acid + mTBD system is shown in Figure 4, and a couple isotherms for the acetic acid + water system are given in Figure 5. As seen in Figure 4, there are large differences between the ePC-SAFT and NRTL model for the acetic acid + mTBD system at low pressures. Protic ILs exhibit a reactive azeotrope, which makes the behavior for these binary systems complex and more difficult to model.[9−11] Additionally, the pressure of the system is generally too low to be measured by most experimental vapor pressure techniques, which accounts for the smaller number of data points in this corner of the composition range. Also, most low pressure vapor pressure techniques rely on measuring mass loss, but for mixtures such as these, this also results in a composition change, and the measurements must be done in a way that allows this to be taken into account. The differences between the models in this region are discussed further in Section 4.3.

The models also allow us to visualize how the pressure changes as the amount of mTBD and acetic acid varies. This is possible because we performed measurements with an excess of acid or base and included mTBD and acetic acid as components in the ePC-SAFT and NRTL models. The results at 350 K are shown in Figure 6. Note that in Figure 6, compositions with lots of mTBD and little water have pressures close to 0 mbar. In general, the pressure is lowest in the range where the concentration of mTBD is the highest, which is reasonable because mTBD has a much lower vapor pressure than water or acetic acid.

For mixtures with the same water content, the lowest pressure generally occurs when there is about the same amount of mTBD and acetic acid, although at high water contents, the minimum occurs where only mTBD and water are present. At the 1:1 composition (x_{acid} of 0.5), almost all of the acid and

https://dx.doi.org/10.1021/acs.jced.9b01039
J. Chem. Eng. Data 2020, 65, 2405−2421

Table 7. Experimental VLE Data for the System Containing Acetic Acid, mTBD, and Water[a]

acetic acid	mTBD	water	Temp. (K)[c]	pressure (mbar)[d]	acetic acid	mTBD	water	Temp. (K)[c]	pressure (mbar)[d]
0.0147	0.0151	0.9702	302.79	41	0	0.2815	0.7185	302.81	20
0.0147	0.0151	0.9702	331.57	185	0.0991	0.1126	0.7883	312.62	42
0.0147	0.0151	0.9702	312.33	74	0.0991	0.1126	0.7883	322.15	70
0.0147	0.0151	0.9702	321.95	117	0.0991	0.1126	0.7883	331.75	114
0.0147	0.0151	0.9702	341.13	281	0.0991	0.1126	0.7883	341.42	178
0.0147	0.0151	0.9702	350.75	420	0.0991	0.1126	0.7883	302.86	25
0.0147	0.0151	0.9702	302.76	45	0.0991	0.1126	0.7883	351.09	261
0.1911	0.1969	0.612	312.41	17	0.4825	0.1257	0.3918	302.78	29
0.1911	0.1969	0.612	321.94	30	0.4825	0.1257	0.3918	312.46	44
0.1911	0.1969	0.612	302.80	10	0.4825	0.1257	0.3918	322.06	67
0.1911	0.1969	0.612	331.73	50	0.4825	0.1257	0.3918	331.56	103
0.1911	0.1969	0.612	341.02	78	0.4825	0.1257	0.3918	341.31	156
0.1911	0.1969	0.612	350.99	124	0.4825	0.1257	0.3918	350.98	231
0.1911	0.1969	0.612	302.81	10	0.084	0.5109	0.4051	312.37	14
0.2004	0.0224	0.7772	312.62	65	0.084	0.5109	0.4051	321.93	23
0.2004	0.0224	0.7772	322.15	107	0.084	0.5109	0.4051	331.52	37
0.2004	0.0224	0.7772	331.75	172	0.084	0.5109	0.4051	302.75	9
0.2004	0.0224	0.7772	341.42	267	0.084	0.5109	0.4051	341.01	58
0.2004	0.0224	0.7772	302.86	38	0.084	0.5109	0.4051	350.69	87
0.2004	0.0224	0.7772	351.09	404	0.3636	0.3537	0.2826	302.79	2
0	0.2053	0.7947	302.72	24	0.3636	0.3537	0.2826	331.57	8
0	0.2053	0.7947	312.26	42	0.3636	0.3537	0.2826	312.33	2
0	0.2053	0.7947	321.71	68	0.3636	0.3537	0.2826	321.95	5
0	0.2053	0.7947	331.12	100	0.3636	0.3537	0.2826	341.13	13
0	0.2053	0.7947	340.73	147	0.3636	0.3537	0.2826	350.75	22
0	0.2053	0.7947	350.44	223	0.3636	0.3537	0.2826	302.76	2
0	0.2053	0.7947	302.69	23	0.0758	0.0754	0.8488	312.27	55
0	0.138	0.862	312.36	52	0.0758	0.0754	0.8488	321.73	89
0	0.138	0.862	321.98	89	0.0758	0.0754	0.8488	302.78	34
0	0.138	0.862	331.45	141	0.0758	0.0754	0.8488	331.42	142
0	0.138	0.862	341.05	221	0.0758	0.0754	0.8488	341.09	220
0	0.138	0.862	302.72	30	0.0758	0.0754	0.8488	350.85	332
0	0.138	0.862	350.74	341	0.0758	0.0754	0.8488	302.94	34
0.155	0.1552	0.6898	302.79	14	0.2188	0.1599	0.6213	321.71	41
0.155	0.1552	0.6898	331.57	72	0.2188	0.1599	0.6213	331.34	71
0.155	0.1552	0.6898	312.33	26	0.2188	0.1599	0.6213	302.78	16
0.155	0.1552	0.6898	321.95	44	0.2188	0.1599	0.6213	312.35	27
0.155	0.1552	0.6898	341.13	114	0.2188	0.1599	0.6213	341.11	114
0.155	0.1552	0.6898	350.75	177	0.2188	0.1599	0.6213	350.67	175
0.155	0.1552	0.6898	302.76	15	0.2188	0.1599	0.6213	302.77	16
0.2967	0.293	0.4103	312.27	7	0.1626	0	0.8374	312.41	65
0.2967	0.293	0.4103	321.73	11	0.1626	0	0.8374	321.94	102
0.2967	0.293	0.4103	302.78	4	0.1626	0	0.8374	302.80	40
0.2967	0.293	0.4103	331.42	17	0.1626	0	0.8374	331.73	163
0.2967	0.293	0.4103	341.09	27	0.1626	0	0.8374	341.02	250
0.2967	0.293	0.4103	350.85	43	0.1626	0	0.8374	350.99	396
0.2967	0.293	0.4103	302.94	4	0.1626	0	0.8374	302.81	46
0.1568	0.3017	0.5415	312.41	19	0.0613	0.1574	0.7813	312.62	41
0.1568	0.3017	0.5415	321.94	32	0.0613	0.1574	0.7813	322.15	68
0.1568	0.3017	0.5415	302.80	16	0.0613	0.1574	0.7813	331.75	109
0.1568	0.3017	0.5415	331.73	51	0.0613	0.1574	0.7813	341.42	169
0.1568	0.3017	0.5415	341.02	77	0.0613	0.1574	0.7813	302.86	24
0.1568	0.3017	0.5415	350.99	115	0.0613	0.1574	0.7813	351.09	255
0.1568	0.3017	0.5415	302.81	15	0.3306	0.2648	0.4047	302.78	8
0.1032	0.1035	0.7933	312.62	45	0.3306	0.2648	0.4047	312.46	12
0.1032	0.1035	0.7933	322.15	74	0.3306	0.2648	0.4047	322.06	19
0.1032	0.1035	0.7933	331.75	119	0.3306	0.2648	0.4047	331.56	29
0.1032	0.1035	0.7933	341.42	188	0.3306	0.2648	0.4047	341.31	44
0.1032	0.1035	0.7933	302.86	26	0.3306	0.2648	0.4047	350.98	67
0.1032	0.1035	0.7933	351.09	287	0	0.7817	0.2183	312.36	6
0.7019	0	0.2981	302.78	40	0	0.7817	0.2183	321.98	11

https://dx.doi.org/10.1021/acs.jced.9b01039
J. Chem. Eng. Data 2020, 65, 2405−2421

Table 7. continued

acetic acid	mTBD	water	Temp. (K)[c]	pressure (mbar)[d]	acetic acid	mTBD	water	Temp. (K)[c]	pressure (mbar)[d]
0.7019	0	0.2981	312.46	65	0	0.7817	0.2183	331.45	20
0.7019	0	0.2981	322.06	104	0	0.7817	0.2183	341.05	34
0.7019	0	0.2981	331.56	161	0	0.7817	0.2183	302.72	3
0.7019	0	0.2981	341.31	246	0	0.7817	0.2183	350.74	54
0.7019	0	0.2981	350.98	364	0	0.7006	0.2994	312.35	20
0.2751	0.301	0.4239	312.37	5	0	0.7006	0.2994	321.94	28
0.2751	0.301	0.4239	321.93	9	0	0.7006	0.2994	331.50	43
0.2751	0.301	0.4239	331.52	16	0	0.7006	0.2994	341.09	67
0.2751	0.301	0.4239	302.75	3	0	0.7006	0.2994	302.72	16
0.2751	0.301	0.4239	341.01	27	0	0.7006	0.2994	350.73	95
0.2751	0.301	0.4239	350.69	44	0	0.7006	0.2994	312.37	21
0.254	0.2556	0.4904	302.79	5	0.893	0.107	0	294.97	9
0.254	0.2556	0.4904	331.57	26	0.893	0.107	0	304.54	15
0.254	0.2556	0.4904	312.33	9	0.893	0.107	0	311.89	22
0.254	0.2556	0.4904	321.95	15	0.893	0.107	0	320.20	34
0.254	0.2556	0.4904	341.13	43	0.893	0.107	0	330.39	56
0.254	0.2556	0.4904	350.75	69	0.893	0.107	0	341.88	94
0.254	0.2556	0.4904	302.76	5	0.893	0.107	0	351.26	139
0.2094	0.2094	0.5811	312.27	14	0.893	0.107	0	312.35	23
0.2094	0.2094	0.5811	321.73	25	0.86	0.14	0	294.97	8
0.2094	0.2094	0.5811	302.78	10	0.86	0.14	0	304.54	12
0.2094	0.2094	0.5811	331.42	44	0.86	0.14	0	311.89	17
0.2094	0.2094	0.5811	341.09	71	0.86	0.14	0	320.20	25
0.2094	0.2094	0.5811	350.85	111	0.86	0.14	0	330.39	40
0.2094	0.2094	0.5811	302.94	10	0.86	0.14	0	341.88	66
0.29	0.1064	0.6037	321.71	71	0.86	0.14	0	351.26	97
0.29	0.1064	0.6037	331.34	117	0.86	0.14	0	312.35	17
0.29	0.1064	0.6037	302.78	27	0.8142	0.1858	0	311.89	3
0.29	0.1064	0.6037	312.35	44	0.8142	0.1858	0	320.20	6
0.29	0.1064	0.6037	341.11	183	0.8142	0.1858	0	330.39	10
0.29	0.1064	0.6037	350.67	276	0.8142	0.1858	0	341.88	17
0.29	0.1064	0.6037	302.77	27	0.8142	0.1858	0	351.26	27
0	0.2815	0.7185	312.41	42	0.8142	0.1858	0	312.35	3
0	0.2815	0.7185	321.94	65	0.9954	0.0046	0	379.15	706[b]
0	0.2815	0.7185	302.80	25	0.9851	0.0149	0	379.04	690[b]
0	0.2815	0.7185	331.73	90	0.9567	0.0433	0	379.07	624[b]
0	0.2815	0.7185	341.02	133	0.9183	0.0817	0	378.87	504[b]
0	0.2815	0.7185	350.99	184					

[a]Compositions are given in mole fractions. Note that the compositions are the total composition in the cell (i.e. PTz data). [b]Measured using the circulation still. All others were measured using the static total pressure apparatus. [c]Expanded uncertainty of the temperature was estimated to be 0.03 K for the static total pressure apparatus and 0.12 K for the circulation still. [d]For the static total pressure apparatus, the standard uncertainty of the pressure was estimated to be 2.3 mbar (expanded uncertainty of 5.6 mbar at the 95% level). For these measurements with the circulation still the expanded uncertainty was estimated to be 20 mbar.

base have reacted to form the IL. Because the IL has a lower vapor pressure than even mTBD, this would explain why a minimum occurs at a 1:1 ratio.

For the most part, this behavior is supported by the experimental data. The experimental points could not be reliably compared visually in Figure 6 because that would require the reader to match lines and dots based on the color shade (a difficult task). Instead, we separately compared the data and model results. The experimental points with an excess of acid always had a higher pressure than comparable points with a 1:1 ratio of acid and base. This was also generally true for the base, and thus, the 1:1 composition generally did exhibit a minimum in the pressure, as described by the ePC-SAFT model. However, at compositions with a large mole fraction of water (more than approximately 0.7), the minimum pressure seems to occur when no acid is present, only mTBD and water. This is correctly shown by the ePC-SAFT in Figure 6, but the problem is the local maximum the model gives between an x_{acid} of 0 and 0.5. This is not supported by the experimental data, even at lower water contents. The experimentally measured pressures in this range fell somewhere between those of the 1:1 composition and the mTBD + water binary.

The NRTL model has more difficulty fitting the data where x_{acid} is about 0.5. It often showed the minimum pressure at a composition with an excess of acid, which largely is due to the fact that the IL component was specified as having that composition. At high water contents, however, the NRTL model even gave a local maximum at an x_{acid} of 0.6. This is not seen in the data and supports the conclusion that the NRTL model had difficulty describing the data in this region.

4.2. Vapor Composition. One of the key uses of VLE data is for designing separation systems, so it is important to know the compositions of the two phases when vaporization occurs.

https://dx.doi.org/10.1021/acs.jced.9b01039
J. Chem. Eng. Data 2020, 65, 2405−2421

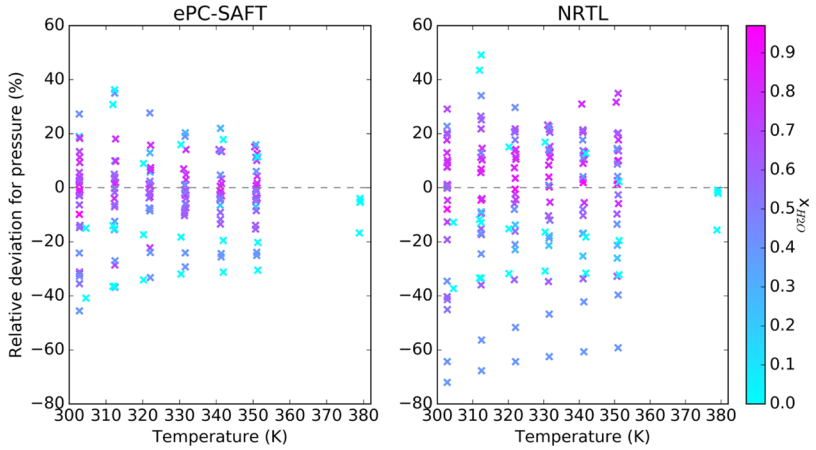

Figure 1. Relative deviation of the ePC-SAFT and NRTL models from the experimental VLE pressure data.

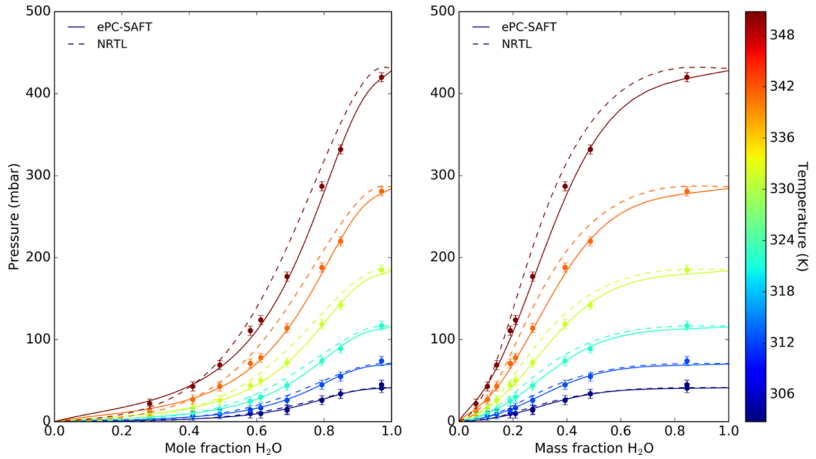

Figure 2. Vapor pressure for the aqueous mTBD acetate system when there is a 1:1 ratio of the acid and base. Left: in terms of mole fraction and right: in terms of mass fraction.

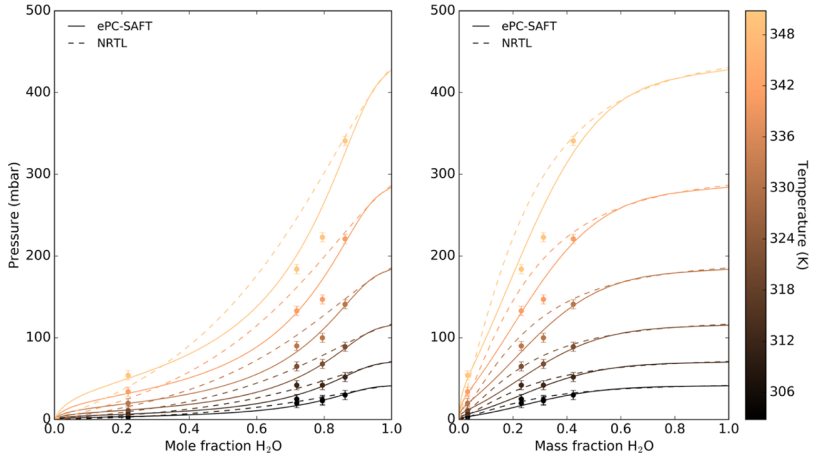

Figure 3. Vapor pressure for mixtures of mTBD and water, with no acetic acid present. Left: in terms of mole fraction and right: in terms of mass fraction.

With the static total pressure apparatus, the vapor composition was not measured, but it can be calculated using the VLE models. To check whether the models accurately calculated the vapor composition, we performed some experiments with a circulation still (see Section 2.4). The experimental data is given in Table 8, and the uncertainties of the concentrations can be found from the data file on the OSF page for this project (https://osf.io/cbe3j/) or in the Supporting Information.

One interesting result from this experiment was that there is approximately the same amount of acid and base in the vapor phase (molar acid to base ratio of 1 or more). It has been shown that with protic ionic liquids the ions will often vaporize disproportionately, leading to an azeotrope with a composition

https://dx.doi.org/10.1021/acs.jced.9b01039
J. Chem. Eng. Data 2020, 65, 2405−2421

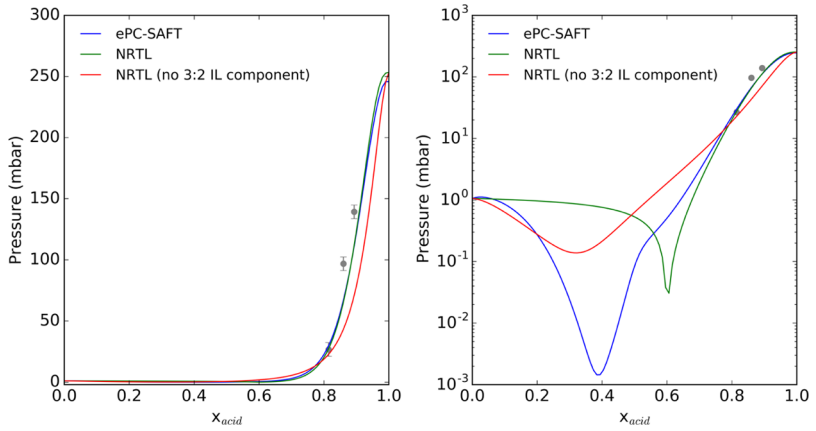

Figure 4. Comparison of different models for the VLE of the mTBD + acetic acid system at 351.2 K.

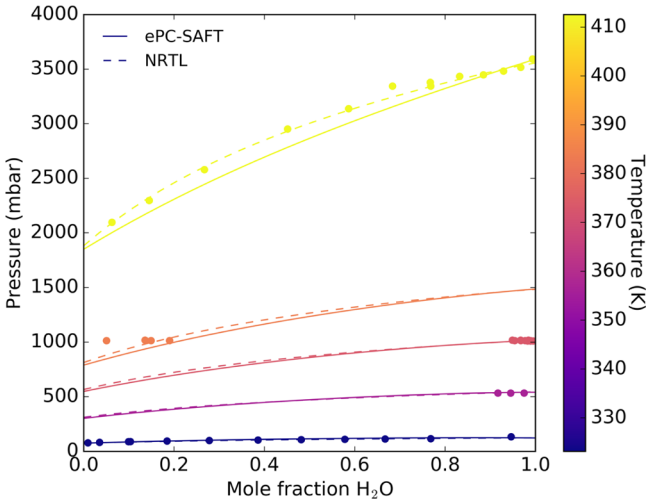

Figure 5. VLE for the acetic acid + water system at selected temperatures. Literature data from refs.[101,108,111,113,115,117,118,120,122,125,126]

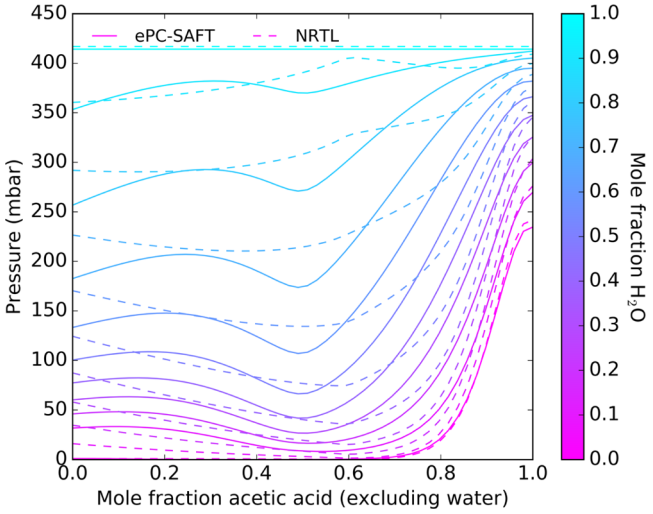

Figure 6. Vapor pressure of the aqueous mTBD acetate system as a function of composition. Temperature set at 350 K.

that is no longer equimolar.[9−12] Indeed, this is the behavior we observed for the system with only mTBD and acetic acid, which is shown in the last two rows of Table 8. The vapor phase contained almost exclusively one component. Hence, for the aqueous mixtures, we were expecting to see more mTBD in the vapor phase than acetic acid. However, our data in Table 8 indicate that in an aqueous solution the vaporization behavior is different and more acid transfers to the vapor phase than would be expected.

Also, hydrolysis occurred in these experiments. mTBD can hydrolyze to form two different products: 1-[3-(methylamino)-propyl]tetrahydro-2(1*H*)-pyrimidinone and 1-(3-aminopropyl)tetrahydro-3-methyl-2(1*H*)-pyrimidinone. No hydrolysis products were detected in the earlier measurements with the static total pressure apparatus, but with the circulation, still hydrolysis did start to occur. We suspect this is due to the higher temperatures used with this setup. Even though the condensation temperatures were similar to temperatures in the static apparatus, the temperature in the reboiler was likely higher.

With this experimental data, we could assess the accuracy of the vapor compositions calculated using the ePC-SAFT and NRTL models. Tables 9 and 10 give values from the ePC-SAFT and NRTL models that can be compared with the experimental results. The models did accurately calculate that the vapor is almost 100% water, but the relative errors for mTBD and acetic acid were quite large. With ePC-SAFT, the values for mTBD were several orders of magnitude smaller than the experimental data, and the ratio of acid to base in the vapor phase was not even close to the 1:1 ratio observed experimentally. With the NRTL model, the reverse was observed: the values for the acetic acid content were extremely small. The deviations from experimental data are much larger than the uncertainty of the experimental methods, so most likely the deviations are due to the models. To better understand these errors and the performance of the models, we compared several different modeling strategies.

4.3. Comparison of Modeling Strategies. There are differences in how the ePC-SAFT and NRTL models behave, as shown in Figure 6. One interesting region is at compositions where there is a mole fraction of about 0.5 acetic acid (on a dry basis). This is where the experimental data usually show a minimum in the pressure. As seen in Figures 6 and 7, the ePC-SAFT model is able to represent this dip in the pressure where x_{acid} is 0.5. The NRTL model, on the other hand, has difficulty in this region.

There are also large differences between the two models at lower water concentrations, as shown in Figures 7 and 4. This seems related to the fact that the ePC-SAFT model gives the

https://dx.doi.org/10.1021/acs.jced.9b01039
J. Chem. Eng. Data 2020, 65, 2405−2421

Table 8. Experimental Data for the Vapor Composition for One Mixture of the Ionic Liquid and Water[b]

		liquid composition (wt %)				vapor composition (wt %)			
T (K)	P (mbar)	water	mTBD	acetic acid	hydro-lyzed mTBD	water	mTBD	acetic acid	acid to base ratio (vapor)
338.02	239	78.3	14.7	5.7	1.3	99.899	0.072	0.029	1.0
347.62	362	78.2	15.7	5.4	0.8	99.968	0.021	0.011	1.4
361.60	633	77.5	15.6	5.6	1.3	99.969	0.021	0.010	1.3
379.07	624	0	10.4	89.7	0	0	0[a]	100.0	
378.87	504	0	18.5	81.5	0	0	0[a]	100.0	

[a]Amount was below the limit of detection of the refractometer, which was 0.037 wt %. [b]Expanded uncertainty of the temperature: 0.12 K; expanded uncertainty of the vapor pressure: 3.8 mbar.

Table 9. Vapor Compositions Predicted Using the ePC-SAFT Model

	experimental				ePC-SAFT					
		Vapor composition (wt %)				vapor composition (wt %)			ratio of calculated to experimental	
T (K)	P (mbar)	water	mTBD	acetic acid	P (mbar)	water	mTBD	acetic acid	mTBD	acetic acid
338.02	239	99.899	0.072	0.029	239	99.918	0.00001	0.082	0.0002	3
347.62	362	99.968	0.021	0.011	364	99.941	0.00005	0.059	0.0025	5
361.60	633	99.969	0.021	0.010	637	99.859	0.00010	0.141	0.0047	14

Table 10. Vapor Compositions Predicted Using the NRTL Model

	experimental				NRTL					
		vapor composition (wt %)				vapor composition (wt %)			ratio of calculated to experimental	
T (K)	P (mbar)	water	mTBD	acetic acid	P (mbar)	water	mTBD	acetic acid	mTBD	acetic acid
338.02	239	99.899	0.072	0.029	248	100.000	0.0004	2×10^{-17}	0.01	5.4×10^{-16}
347.62	362	99.968	0.021	0.011	375	99.999	0.001	1×10^{-16}	0.04	8.8×10^{-15}
361.60	633	99.969	0.021	0.010	657	99.999	0.001	1×10^{-15}	0.07	1.1×10^{-13}

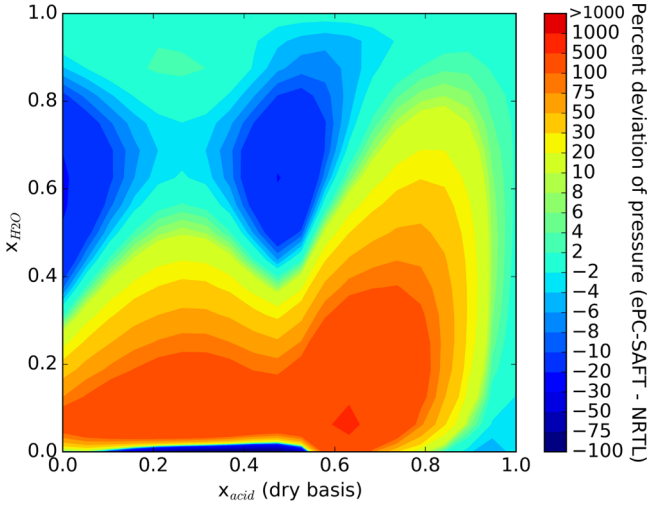

Figure 7. Comparison of the relative deviation between the ePC-SAFT and NRTL models at 351 K.

wrong behavior for the binary system containing only acetic acid and mTBD. When comparing the results, the ePC-SAFT model gives a minimum, where x_{acid} equals 0.39 for the binary system. This is wrong because, as earlier studies have shown, for these types of protic ionic liquids, the minimum (azeotrope) occurs at compositions where there is more acid than base.[9−11] This was the reason that the IL component in the NRTL model was defined to have a composition with more acid, and including this separate component essentially keeps the minimum for the acid + base binary at a reasonable composition.

Using the 3:2 IL component in the NRTL model also led to the differences observed in vapor composition. As mentioned, for aqueous solutions with approximately the same amount of acid and base (x_{acid} of 0.5), the ePC-SAFT model predicted almost no mTBD in the vapor phase and the NRTL model predicted almost no acetic acid. Because the IL component in the NRTL model was set to have a composition of 3 acid molecules and 2 base molecules (x_{acid} of 0.6), for mixtures, where x_{acid} was 0.5 the model gave an excess of base in the mixture. The vapor pressure of the 3:2 IL component was much lower than that of mTBD, and no acetic acid was present (due to the simple reaction scheme used), and this led to the extremely low acid content in the vapor phase for aqueous mixtures. In contrast, the reaction equation used with the ePC-SAFT model allowed for some unreacted acetic acid, and because acetic acid has a much higher vapor pressure than mTBD or the ions, it was the main compound that appeared in the vapor phase (besides water).

We also tested different optimization procedures to see if it would be possible to find a set of parameters that would give better results for the vapor composition. For instance, we tried including the data from the circulation still and reoptimizing, but large errors in the vapor composition still persisted. We also found that including vapor composition data in the optimization affected both the NRTL and ePC-SAFT models, leading to poorer prediction of the vapor pressure. We also tried optimizing by adding a large weight to the error of the vapor composition. The model then provided reasonable values for the composition of the vapor, but the pressures

https://dx.doi.org/10.1021/acs.jced.9b01039
J. Chem. Eng. Data 2020, 65, 2405−2421

calculated were much lower than they should have been. This indicates that the models, as currently formulated, cannot accurately describe the vapor composition of the aqueous IL mixtures without being contorted in a way that damages the models' overall performance.

Because the structure of the model affects its performance, we also tested a few other modeling strategies, and a summary of the comparison is given in Table 11. We attempted using a simpler NRTL model that only had water, acetic acid, and mTBD as components (no IL component). However, this model could not accurately represent the drop in pressure around x_{acid} compositions of about 0.5, and it gave poor results. It seems that because the system is complicated, involving reactions and association interactions, a model with more components, or at least more parameters, is needed.

Table 11. Comparison of Different Strategies for Modeling the VLE of Aqueous Ionic Liquid Systems

NRTL (no IL component)	ePC-SAFT
•few fitted parameters (we used 8)	•gives accurate values for VLE pressure
•no need to specify extra IL component	•more physically correct (uses ions instead of molecular IL component)
•could not describe VLE behavior well	•can also calculate densities
	•more fitted parameters than NRTL (we used 17)
	•more complicated structure than NRTL
NRTL	**ePC-SAFT (with OH^-)**
•fewer parameters than ePC-SAFT (we used 8)	•more similar to actual system because mTBD reacts with water
•no need to solve for roots	•more parameters needed, which can cause overfitting
•gives accurate values for VLE pressure	•increased complexity led to unreliable results in many regions
•must specify reasonable IL component	
•fixed IL component stoichiometry makes model less flexible	

We also tried an NRTL model that included the interaction parameters between mTBD and the IL component. This added two more parameters to the model and did allow the model to provide a slightly better fit: the root mean squared error was 23%, instead of 24% for the main model presented here that did not include those interaction parameters. However, these additional interaction parameters also led to sharp jumps in the pressure at x_{acid} compositions close to 0.6.

We tested some more complex ePC-SAFT models as well because mTBD also reacts with water. Including this reaction, and the resulting hydroxide ion, did not improve the model. Using an additional compound adds many additional parameters, and this increased complexity resulted in overfitting. We calculated densities and vapor pressures across the full range of compositions, and although near data points, the model gave reasonable values, and in areas between data points, large jumps in the pressure and density were observed. In summary, including the hydroxide ion made the model unreliable because it was too complex.

It was also possible to get good results when defining a separate IL component in the PC-SAFT model, as was done with the NRTL model, that is, instead of using electrolyte PC-SAFT, the IL was defined as a molecular species and the electrolyte term was not included. Similar jumps in the pressure were also observed when including an additional component for 7-methyl-1,5,7-triazabicyclo[4.4.0]dec-5-enium hydroxide.

5. CONCLUSIONS

Based on the experimental VLE data, we observed that the vapor pressure of the aqueous IL system decreases as the amount of mTBD increases. This is logical because mTBD has a lower vapor pressure than acetic acid or water. The minimum pressure, for a given water content, generally occurs where there is an equimolar amount of acid and base. At that point, most of the acid and base have reacted to form the ionic liquid, which has a very low vapor pressure. Although previous studies have shown that protic ionic liquids have a minimum in pressure at more acidic compositions when no water is present, based on data from this article, it seems that for aqueous mixtures, the minimum pressure occurs at an equimolar ratio of acid and base.

The VLE behavior is complex, and modeling it is challenging. It was possible to model the VLE pressures across the full range of acid and base concentrations using both the ePC-SAFT and NRTL models. With the NRTL model, we needed to define a separate IL component to be able to describe the VLE pressures accurately. However, it was not possible for the models to accurately predict the vapor composition in the system. Either the acid or base composition was several orders of magnitude smaller than expected. There were also some areas where the two models diverged, which highlights some of the differences in the models and in what components and parameter sets were used with the models.

■ ASSOCIATED CONTENT

Supporting Information

The Supporting Information is available free of charge at https://pubs.acs.org/doi/10.1021/acs.jced.9b01039.

Data file containing all the experimental data for this article (XLS)

■ AUTHOR INFORMATION

Corresponding Author

Petri Uusi-Kyyny − *Department of Chemical and Metallurgical Engineering, Aalto University, FI-00076 Aalto, Finland;* orcid.org/0000-0002-8339-4601; Email: petri.uusi-kyyny@aalto.fi

Authors

Zachariah Steven Baird − *Department of Chemical and Metallurgical Engineering, Aalto University, FI-00076 Aalto, Finland;* orcid.org/0000-0002-4327-3469

Joanna Witos − *Department of Bioproducts and Biosystems, Aalto University, FI-00076 Aalto, Finland*

Antti H. Rantamäki − *Department of Chemistry, University of Helsinki, FI-00014 Helsinki, Finland*

Herbert Sixta − *Department of Bioproducts and Biosystems, Aalto University, FI-00076 Aalto, Finland;* orcid.org/0000-0002-9884-6885

Susanne K. Wiedmer − *Department of Chemistry, University of Helsinki, FI-00014 Helsinki, Finland;* orcid.org/0000-0002-3097-6165

Ville Alopaeus − *Department of Chemical and Metallurgical Engineering, Aalto University, FI-00076 Aalto, Finland*

Complete contact information is available at:

https://dx.doi.org/10.1021/acs.jced.9b01039
J. Chem. Eng. Data 2020, 65, 2405−2421

https://pubs.acs.org/10.1021/acs.jced.9b01039

Notes

The authors declare no competing financial interest.

■ ACKNOWLEDGMENTS

Funding was provided by Business Finland (grant no. 560/31/2017).

■ REFERENCES

(1) Parviainen, A.; King, A. W. T.; Mutikainen, I.; Hummel, M.; Selg, C.; Hauru, L. K. J.; Sixta, H.; Kilpeläinen, I. Predicting Cellulose Solvating Capabilities of Acid−Base Conjugate Ionic Liquids. *ChemSusChem* **2013**, *6*, 2161−2169.

(2) Parviainen, A.; Wahlström, R.; Liimatainen, U.; Liitiä, T.; Rovio, S.; Helminen, J. K. J.; Hyväkkö, U.; King, A. W. T.; Suurnäkki, A.; Kilpeläinen, I. Sustainability of Cellulose Dissolution and Regeneration in 1,5-Diazabicyclo[4.3.0]Non-5-Enium Acetate: A Batch Simulation of the IONCELL-F Process. *RSC Adv.* **2015**, *5*, 69728−69737.

(3) Shamshina, J. L.; Barber, P. S.; Gurau, G.; Griggs, C. S.; Rogers, R. D. Pulping of Crustacean Waste Using Ionic Liquids: To Extract or Not To Extract. *ACS Sustainable Chem. Eng.* **2016**, *4*, 6072−6081.

(4) Kuroda, K.; Kunimura, H.; Fukaya, Y.; Nakamura, N.; Ohno, H. 1H NMR Evaluation of Polar and Nondeuterated Ionic Liquids for Selective Extraction of Cellulose and Xylan from Wheat Bran. *ACS Sustainable Chem. Eng.* **2014**, *2*, 2204−2210.

(5) Sixta, H.; Hummel, M.; Le, B. K.; Kilpeläinen, I.; King, A. W. T.; Helminen, K. J. J.; Hellstén, S. A Process for Making a Cellulose Fibre or Film. WO 2018138416 A1, August 2, 2018.

(6) Kazakov, A.; Magee, J. W.; Chirico, R. D.; Paulechka, E.; Diky, V.; Muzny, C. D.; Kroenlein, K.; Frenkel, M. Ionic Liquids Database - ILThermo. https://ilthermo.boulder.nist.gov/ (accessed Nov 8, 2018).

(7) Ostonen, A.; Uusi-Kyyny, P.; Pakkanen, M.; Alopaeus, V. Dew Points of Pure DBN and DBU and Vapor−Liquid Equilibria of Water +DBN and Water+DBU Systems for Cellulose Solvent Recycling. *Fluid Phase Equilib.* **2016**, *408*, 79−87.

(8) George, A.; Brandt, A.; Tran, K.; Zahari, S. M. S. N. S.; Klein-Marcuschamer, D.; Sun, N.; Sathitsuksanoh, N.; Shi, J.; Stavila, V.; Parthasarathi, R.; Singh, S.; Holmes, B. M.; Welton, T.; Simmons, B. A.; Hallett, J. P. Design of Low-Cost Ionic Liquids for Lignocellulosic Biomass Pretreatment. *Green Chem.* **2015**, *17*, 1728−1734.

(9) Ribeiro, F. M. S.; Lima, C. F. R. A. C.; Silva, A. M. S.; Santos, L. M. N. B. F. Experimental Evidence for Azeotrope Formation from Protic Ionic Liquids. *ChemPhysChem* **2018**, *19*, 2364−2369.

(10) Lopes, J. N. C.; Rebelo, L. P. N. Ionic Liquids and Reactive Azeotropes: The Continuity of the Aprotic and Protic Classes. *Phys. Chem. Chem. Phys.* **2010**, *12*, 1948−1952.

(11) Ahmad, W.; Ostonen, A.; Jakobsson, K.; Uusi-Kyyny, P.; Alopaeus, V.; Hyväkkö, U.; King, A. W. T. Feasibility of Thermal Separation in Recycling of the Distillable Ionic Liquid [DBNH][OAc] in Cellulose Fiber Production. *Chem. Eng. Res. Des.* **2016**, *114*, 287−298.

(12) Greaves, T. L.; Drummond, C. J. Protic Ionic Liquids: Evolving Structure−Property Relationships and Expanding Applications. *Chem. Rev.* **2015**, *115*, 11379−11448.

(13) Wijaya, E. C.; Separovic, F.; Drummond, C. J.; Greaves, T. L. Stability and Activity of Lysozyme in Stoichiometric and Non-Stoichiometric Protic Ionic Liquid (PIL)-Water Systems. *J. Chem. Phys.* **2018**, *148*, 193838.

(14) Mazaheripour, A.; Majumdar, S.; Hanemann-Rawlings, D.; Thomas, E. M.; McGuiness, C.; d'Alencon, L.; Chabinyc, M. L.; Segalman, R. A. Tailoring the Seebeck Coefficient of PEDOT:PSS by Controlling Ion Stoichiometry in Ionic Liquid Additives. *Chem. Mater.* **2018**, *30*, 4816−4822.

(15) Renon, H.; Prausnitz, J. M. Local Compositions in Thermodynamic Excess Functions for Liquid Mixtures. *AIChE J.* **1968**, *14*, 135−144.

(16) Renon, H.; Prausnitz, J. M. Estimation of Parameters for the NRTL Equation for Excess Gibbs Energies of Strongly Nonideal Liquid Mixtures. *Ind. Eng. Chem. Process Des. Dev.* **1969**, *8*, 413−419.

(17) Wilson, G. M. Vapor-Liquid Equilibrium. XI. A New Expression for the Excess Free Energy of Mixing. *J. Am. Chem. Soc.* **1964**, *86*, 127−130.

(18) Held, C.; Reschke, T.; Mohammad, S.; Luza, A.; Sadowski, G. EPC-SAFT Revised. *Chem. Eng. Res. Des.* **2014**, *92*, 2884−2897.

(19) Klamt, A. Conductor-like Screening Model for Real Solvents: A New Approach to the Quantitative Calculation of Solvation Phenomena. *J. Phys. Chem.* **1995**, *99*, 2224−2235.

(20) Maurer, G.; Prausnitz, J. M. On the Derivation and Extension of the Uniquac Equation. *Fluid Phase Equilib.* **1978**, *2*, 91−99.

(21) Chen, C.-C.; Britt, H. I.; Boston, J. F.; Evans, L. B. Local Composition Model for Excess Gibbs Energy of Electrolyte Systems. Part I: Single Solvent, Single Completely Dissociated Electrolyte Systems. *AIChE J.* **1982**, *28*, 588−596.

(22) Fredenslund, A.; Jones, R. L.; Prausnitz, J. M. Group-Contribution Estimation of Activity Coefficients in Nonideal Liquid Mixtures. *AIChE J.* **1975**, *21*, 1086−1099.

(23) Chapman, W. G.; Gubbins, K. E.; Jackson, G.; Radosz, M. SAFT: Equation-of-State Solution Model for Associating Fluids. *Fluid Phase Equilib.* **1989**, *52*, 31−38.

(24) Ji, X.; Held, C.; Sadowski, G. Modeling Imidazolium-Based Ionic Liquids with EPC-SAFT. *Fluid Phase Equilib.* **2012**, *335*, 64−73.

(25) Simoni, L. D.; Ficke, L. E.; Lambert, C. A.; Stadtherr, M. A.; Brennecke, J. F. Measurement and Prediction of Vapor−Liquid Equilibrium of Aqueous 1-Ethyl-3-Methylimidazolium-Based Ionic Liquid Systems. *Ind. Eng. Chem. Res.* **2010**, *49*, 3893−3901.

(26) Ji, X.; Held, C.; Sadowski, G. Modeling Imidazolium-Based Ionic Liquids with EPC-SAFT. Part II. Application to H2S and Synthesis-Gas Components. *Fluid Phase Equilib.* **2014**, *363*, 59−65.

(27) Simoni, L. D.; Lin, Y.; Brennecke, J. F.; Stadtherr, M. A. Modeling Liquid−Liquid Equilibrium of Ionic Liquid Systems with NRTL, Electrolyte-NRTL, and UNIQUAC. *Ind. Eng. Chem. Res.* **2008**, *47*, 256−272.

(28) Baird, Z. S.; Dahlberg, A.; Uusi-Kyyny, P.; Osmanbegovic, N.; Witos, J.; Helminen, J.; Cederkrantz, D.; Hyväri, P.; Alopaeus, V.; Kilpeläinen, I.; Wiedmer, S. K.; Sixta, H. Physical Properties of 7-Methyl-1,5,7-Triazabicyclo[4.4.0]Dec-5-Ene (MTBD). *Int. J. Thermophys.* **2019**, *40*, 71.

(29) Turkia, H.; Sirén, H.; Pitkänen, J.-P.; Wiebe, M.; Penttilä, M. Capillary Electrophoresis for the Monitoring of Carboxylic Acid Production by Gluconobacter Oxydans. *J. Chromatogr. A* **2010**, *1217*, 1537−1542.

(30) Wagner, W.; Pruß, A. The IAPWS Formulation 1995 for the Thermodynamic Properties of Ordinary Water Substance for General and Scientific Use. *J. Phys. Chem. Ref. Data* **2002**, *31*, 387−535.

(31) Yerazunis, S.; Plowright, J. D.; Smola, F. M. Vapor-liquid Equilibrium Determination by a New Apparatus. *AIChE J.* **1964**, *10*, 660−665.

(32) Uusi-Kyyny, P.; Pokki, J.-P.; Aittamaa, J.; Liukkonen, S. Vapor−Liquid Equilibrium for the Binary Systems of 3-Methylpentane + 2-Methyl-2-Propanol at 331 K and + 2-Butanol at 331 K. *J. Chem. Eng. Data* **2001**, *46*, 754−758.

(33) Sapei, E.; Zaytseva, A.; Uusi-Kyyny, P.; Keskinen, K. I.; Aittamaa, J. Vapor−Liquid Equilibrium for Binary System of Thiophene+2,2,4-Trimethylpentane at 343.15 and 353.15K and Thiophene+2-Ethoxy-2-Methylpropane at 333.15 and 343.15K. *Fluid Phase Equilib.* **2007**, *261*, 115−121.

(34) Cameretti, L. F.; Sadowski, G.; Mollerup, J. M. Modeling of Aqueous Electrolyte Solutions with Perturbed-Chain Statistical Associated Fluid Theory. *Ind. Eng. Chem. Res.* **2005**, *44*, 3355−3362.

(35) Gross, J.; Sadowski, G. Perturbed-Chain SAFT: An Equation of State Based on a Perturbation Theory for Chain Molecules. *Ind. Eng. Chem. Res.* **2001**, *40*, 1244−1260.

(36) Gross, J.; Sadowski, G. Application of the Perturbed-Chain SAFT Equation of State to Associating Systems. *Ind. Eng. Chem. Res.* **2002**, *41*, 5510−5515.
(37) Huang, S. H.; Radosz, M. Equation of State for Small, Large, Polydisperse, and Associating Molecules. *Ind. Eng. Chem. Res.* **1990**, *29*, 2284−2294.
(38) Huang, S. H.; Radosz, M. Equation of State for Small, Large, Polydisperse, and Associating Molecules: Extension to Fluid Mixtures. *Ind. Eng. Chem. Res.* **1991**, *30*, 1994−2005.
(39) Huang, S. H.; Radosz, M. Equation of State for Small, Large, Polydisperse, and Associating Molecules: Extension to Fluid Mixtures. [Erratum to Document Cited in CA115(8):79950j]. *Ind. Eng. Chem. Res.* **1993**, *32*, 762.
(40) Chapman, W. G.; Gubbins, K. E.; Jackson, G.; Radosz, M. New Reference Equation of State for Associating Liquids. *Ind. Eng. Chem. Res.* **1990**, *29*, 1709−1721.
(41) Archer, D. G.; Wang, P. The Dielectric Constant of Water and Debye-Hückel Limiting Law Slopes. *J. Phys. Chem. Ref. Data* **1990**, *19*, 371−411.
(42) *DIPPR Project 801—Full Version*; Design Institute For Physical Properties.
(43) Weingärtner, H. The Static Dielectric Permittivity of Ionic Liquids. *J. Mol. Liq.* **2014**, *192*, 185−190.
(44) Dahm, K. D.; Visco, D. P. *Fundamentals of Chemical Engineering Thermodynamics*; Cengage Learning, 2014.
(45) *Van't Hoff Equation*; Wikipedia, 2019.
(46) Ostonen, A.; Bervas, J.; Uusi-Kyyny, P.; Alopaeus, V.; Zaitsau, D. H.; Emel'yanenko, V. N.; Schick, C.; King, A. W. T.; Helminen, J.; Kilpeläinen, I.; Khachatrian, A. A.; Varfolomeev, M. A.; Verevkin, S. P. Experimental and Theoretical Thermodynamic Study of Distillable Ionic Liquid 1,5-Diazabicyclo[4.3.0]Non-5-Enium Acetate. *Ind. Eng. Chem. Res.* **2016**, *55*, 10445−10454.
(47) Ostonen, A. *Thermodynamic Study of Protic Ionic Liquids*; Aalto University, 2017.
(48) Ishikawa, T. *Superbases for Organic Synthesis: Guanidines, Amidines, Phosphazenes and Related Organocatalysts*; John Wiley & Sons, 2009.
(49) Heisler, I. A.; Mazur, K.; Meech, S. R. Hydroxide Hydrogen Bonding: Probing the Solvation Structure through Ultrafast Time Domain Raman Spectroscopy. *J. Phys. Chem. Lett.* **2011**, *2*, 1155−1160.
(50) Rabideau, B. D.; Ismail, A. E. Mechanisms of hydrogen bond formation between ionic liquids and cellulose and the influence of water content. *Phys. Chem. Chem. Phys.* **2015**, *17*, 5767−5775.
(51) Greaves, T. L.; Drummond, C. J. Protic Ionic Liquids: Properties and Applications. *Chem. Rev.* **2008**, *108*, 206−237.
(52) Uyan, M.; Sieder, G.; Ingram, T.; Held, C. Predicting CO2 Solubility in Aqueous N-Methyldiethanolamine Solutions with EPC-SAFT. *Fluid Phase Equilib.* **2015**, *393*, 91−100.
(53) Cameretti, L. F.; Sadowski, G. Modeling of Aqueous Amino Acid and Polypeptide Solutions with PC-SAFT. *Chem. Eng. Process.* **2008**, *47*, 1018−1025.
(54) Kiepe, J.; Karine de Araújo Rodrigues, A.; Horstmann, S.; Gmehling, J. Experimental Determination and Correlation of Liquid Density Data of Electrolyte Mixtures Containing Water or Methanol. *Ind. Eng. Chem. Res.* **2003**, *42*, 2022−2029.
(55) Robinson, R. A.; Stokes, R. H. *Electrolyte Solutions: Second Revised Edition*; Dover Publications, 1959.
(56) Nasirzadeh, K.; Neueder, R.; Kunz, W. Vapor Pressures and Osmotic Coefficients of Aqueous LiOH Solutions at Temperatures Ranging from 298.15 to 363.15 K. *Ind. Eng. Chem. Res.* **2005**, *44*, 3807−3814.
(57) Pitzer, K. S.; Peiper, J. C.; Busey, R. H. Thermodynamic Properties of Aqueous Sodium Chloride Solutions. *J. Phys. Chem. Ref. Data* **1984**, *13*, 1−102.
(58) Gibbard, H. F.; Scatchard, G. Liquid-Vapor Equilibrium of Aqueous Lithium Chloride, from 25 to 100.Deg. and from 1.0 to 18.5 Molal, and Related Properties. *J. Chem. Eng. Data* **1973**, *18*, 293−298.
(59) Platford, R. F. Osmotic Coefficients of Aqueous Solutions of Seven Compounds at 0.Deg. *J. Chem. Eng. Data* **1973**, *18*, 215−217.
(60) Apelblat, A.; Manzurola, E. Volumetric and thermal properties of some aqueous electrolyte solutions. *J. Mol. Liq.* **2005**, *118*, 77−88.
(61) Apelblat, A.; Manzurola, E. Volumetric Properties of Aqueous Solutions of Sodium Bromide at Temperatures from 278.15 K to 338.15 K and Molalities of (0.1, 0.5, and 1.0) Mol · Kg−1. *J. Chem. Thermodyn.* **2001**, *33*, 581−595.
(62) Apelblat, A.; Manzurola, E. Volumetric Properties of Water, and Solutions of Sodium Chloride and Potassium Chloride at Temperatures FromT= 277.15 K ToT= 343.15 K at Molalities of (0.1, 0.5, and 1.0)Mol·kg−1. *J. Chem. Thermodyn.* **1999**, *31*, 869−893.
(63) Apelblat, A.; Manzurola, E. Volumetric Properties of Aqueous Solutions of Lithium Chloride at Temperatures from 278.15 K to 338.15 K and Molalities (0.1, 0.5, and 1.0)Mol · Kg−1. *J. Chem. Thermodyn.* **2001**, *33*, 1133−1155.
(64) Campbell, A. N.; Bhatnagar, O. N. Osmotic and Activity Coefficients of Sodium Hydroxide in Water from 150 to 250.Degree.C. *J. Chem. Eng. Data* **1984**, *29*, 166−168.
(65) Corti, H. R.; Simonson, J. M. Densities and Apparent Molar Volumes of NaOH(Aq) to the Temperature 623 K and Pressure to 30 MPa. *J. Solution Chem.* **2006**, *35*, 1057−1074.
(66) Herrington, T. M.; Pethybridge, A. D.; Roffey, M. G. Densities of Aqueous Lithium, Sodium and Potassium Hydroxides from 25 to 75.Degree. C at 1 Atm. *J. Chem. Eng. Data* **1986**, *31*, 31−34.
(67) Kelly, W. R.; Borza, P. F.; Harriger, R. D. Densities and Viscosities of Potassium Hydroxide Solutions at Low Temperatures. *J. Chem. Eng. Data* **1965**, *10*, 233−234.
(68) Gu, F.; Hou, Y. Salt Effects on the Isobaric Vapor−Liquid Equilibrium for Four Binary Systems. *J. Chem. Eng. Data* **2000**, *45*, 467−470.
(69) Vercher, E.; Orchillés, A. V.; Vázquez, M. I.; Martínez-Andreu, A. Isobaric Vapor−Liquid Equilibria for Water + Acetic Acid + Potassium Acetate. *J. Chem. Eng. Data* **2004**, *49*, 566−569.
(70) Venkatesu, P.; Lee, M.-J.; Lin, H.-m. Densities of Aqueous Solutions Containing Model Compounds of Amino Acids and Ionic Salts at T=298.15K. *J. Chem. Thermodyn.* **2007**, *39*, 1206−1216.
(71) Banipal, T. S.; Singh, K.; Banipal, P. K.; Sood, A. K.; Singh, P.; Singh, G.; Patyar, P. Volumetric and Viscometric Studies of Some Metal Acetates in Aqueous Solutions at T = (288.15 to 318.15) K. *J. Chem. Eng. Data* **2008**, *53*, 2758−2765.
(72) Terdale, S.; Dagade, D.; Patil, K. Activity Coefficient Studies in Ternary Aqueous Solutions at 298.15 K: H2O + α-Cyclodextrin + Potassium Acetate and H2O + 18-Crown-6 + Hydroquinone Systems. *J. Chem. Eng. Data* **2009**, *54*, 294−300.
(73) Terdale, S.; Dagade, D.; Patil, K. Activity Coefficient Studies in Ternary Aqueous Solutions at 298.15 K: H2O + α-Cyclodextrin + Potassium Acetate and H2O + 18-Crown-6 + Hydroquinone Systems. *J. Chem. Eng. Data* **2009**, *54*, 1956.
(74) Taha, M.; Lee, M. -J. Volumetric Properties of MES, MOPS, MOPSO, and MOBS in Water and in Aqueous Electrolyte Solutions. *Thermochim. Acta* **2010**, *505*, 86−97.
(75) Chmielewska, A.; Wypych-Stasiewicz, A.; Bald, A. Viscosimetric Studies of Aqueous Solutions of Salts of Carboxylic Acids. *J. Mol. Liq.* **2005**, *122*, 110−115.
(76) Kharat, S. J. Density, Viscosity and Ultrasonic Velocity Studies of Aqueous Solutions of Sodium Acetate at Different Temperatures. *J. Mol. Liq.* **2008**, *140*, 10−14.
(77) Banipal, T. S.; Kahlon, G. K.; Kaur, J.; Singh, K.; Mehra, V.; Chawla, R.; Banipal, P. K. Volumetric Properties of Some α,ω-Aminocarboxylic Acids in Aqueous Sodium Acetate and Magnesium Acetate Solutions at T = (288.15 to 318.15) K. *J. Chem. Eng. Data* **2010**, *55*, 4864−4871.
(78) Bochmann, S.; May, P. M.; Hefter, G. Molar Volumes and Heat Capacities of Aqueous Solutions of Short-Chain Aliphatic Sodium Carboxylates at 25 °C. *J. Chem. Eng. Data* **2011**, *56*, 5081−5087.
(79) Beyer, R.; Steiger, M. Vapour Pressure Measurements and Thermodynamic Properties of Aqueous Solutions of Sodium Acetate. *J. Chem. Thermodyn.* **2002**, *34*, 1057−1071.

https://dx.doi.org/10.1021/acs.jced.9b01039
J. Chem. Eng. Data 2020, 65, 2405−2421

(80) Vercher, E.; Vázquez, M. I.; Martínez-Andreu, A. Isobaric Vapor−Liquid Equilibria for Water + Acetic Acid + Lithium Acetate. *J. Chem. Eng. Data* **2001**, *46*, 1584−1588.
(81) Apelblat, A.; Korin, E. The Vapour Pressures of Saturated Aqueous Solutions of Sodium Chloride, Sodium Bromide, Sodium Nitrate, Sodium Nitrite, Potassium Iodate, and Rubidium Chloride at Temperatures from 227 K to 323 K. *J. Chem. Thermodyn.* **1998**, *30*, 59−71.
(82) Meranda, D.; Furter, W. F. Elevation of the Boiling Point of Water by Salts at Saturation: Data and Correlation. *J. Chem. Eng. Data* **1977**, *22*, 315−317.
(83) Mashovets, V. P.; Zarembo, V. I.; Fedorov, M. K. Vapor Pressure of Aqueous NaCl, NaBr, and NaI at Temperatures from 150-350 C. *Zh. Prikl. Khim.* **1973**, *3*, 651−652.
(84) Zarembo, V. I.; Antonov, N. A.; Gilyarov, V. N.; Fedorov, M. K. Activity Coefficients KCl in the System KCl-H2O at Temperatures from 150 to 350 and at Pressures to 1500 Kg/Cm2. *Zh. Prikl. Khim.* **1976**, *46*, 1221−1225.
(85) Spiro, N. S. Correlation between Concentration and Pressure in Saturated Aqueous Salt Solutions. *Zh. Fiz. Khim.* **1962**, *36*, 2256−2261.
(86) Kiepe, J.; Horstmann, S.; Fischer, K.; Gmehling, J. Experimental Determination and Prediction of Gas Solubility Data for Methane + Water Solutions Containing Different Monovalent Electrolytes. *Ind. Eng. Chem. Res.* **2003**, *42*, 5392−5398.
(87) Sada, E.; Morisue, T.; Miyahara, K. Salt Effects On Vapor-Liquid Equilibrium Of Isopropanol-Water System. *J. Chem. Eng. Jpn.* **1975**, *8*, 196−201.
(88) Lee, L.-s.; Lee, C.-c. Vapor Pressures and Enthalpies of Vaporization of Aqueous Solutions of Benzyltrimethylammonium Chloride, Benzyltriethylammonium Chloride, and Benzltributylammonium Chloride. *J. Chem. Eng. Data* **1998**, *43*, 17−20.
(89) Lee, L.-s.; Lee, C.-c. Vapor Pressures and Enthalpies of Vaporization of Aqueous Solutions of Triethylammonium Chloride, 2-Hydroxyethylammonium Chloride, and Tris(Hydroxymethyl)-Aminomethane Hydrochloride. *J. Chem. Eng. Data* **1998**, *43*, 469−472.
(90) Chaudhari, S. K.; Patil, K. R. Thermodynamic Properties of Aqueous Solutions of Lithium Chloride. *Phys. Chem. Liq.* **2002**, *40*, 317−325.
(91) Wei, D.; Lu, J.; Zhu, J.; Zhou, X. THE STUDIES ON SALT EFFECT OF THE ISOTHERMAL VAPOUR-LIQUID EQUILIBRIUM——ORGANIC SOLVENT-WATER-INORGANIC SALT SYSTEM. *Acta Phys.-Chim. Sin.* **1987**, *3*, 520−524.
(92) Hsu, H.-l.; Wu, Y.-c.; Lee, L.-s. Vapor Pressures of Aqueous Solutions with Mixed Salts of NaCl + KBr and NaBr + KCl. *J. Chem. Eng. Data* **2003**, *48*, 514−518.
(93) Clarke, E. C. W.; Glew, D. N. Evaluation of the Thermodynamic Functions for Aqueous Sodium Chloride from Equilibrium and Calorimetric Measurements below 154 °C. *J. Phys. Chem. Ref. Data* **1985**, *14*, 489−610.
(94) Broul, M.; Hlavatý, K.; Linek, J. Liquid-Vapour Equilibrium in Systems of Electrolytic Components: V the System Methanol + Water + Lithium Chloride at 60 c. *Collect. Czech. Chem. Commun.* **1969**, *34*, 3428.
(95) Hamer, W. J.; Wu, Y. C. Osmotic Coefficients and Mean Activity Coefficients of Uni-univalent Electrolytes in Water at 25°C. *J. Phys. Chem. Ref. Data* **1972**, *1*, 1047−1100.
(96) Holmes, H. F.; Mesmer, R. E. Isopiestic Molalities for Aqueous Solutions of the Alkali Metal Hydroxides at Elevated Temperatures. *J. Chem. Thermodyn.* **1998**, *30*, 311−326.
(97) Achary, M. V. R.; Rao, M. N. Vapor-Liquid Equilibrium of Non-Ideal Solutions. *Trans., Indian Inst. Chem. Eng.* **1947**, *29*, 1.
(98) Apelblat, A.; Manzurola, E. Excess Molar Volumes of Formic Acid+ Water Acetic Acid+ Water and Propionic Acid+ Water Systems at 288.15, 298.15 and 308.15 K. *Fluid Phase Equilib.* **1987**, *32*, 163−193.
(99) Bald, A.; Kinart, Z. Volumetric Properties of Some Aliphatic Mono-and Dicarboxylic Acids in Water at 298.15 K. *J. Solution Chem.* **2011**, *40*, 1−16.
(100) Bennett, G. W. A Laboratory Experiment on the Boiling-Point Curves of Non-Azeotropic Binary Mixtures. *J. Chem. Educ.* **1929**, *6*, 1544.
(101) Bernatová, S.; Aim, K.; Wichterle, I. Isothermal Vapour−Liquid Equilibrium with Chemical Reaction in the Quaternary Water + Methanol+ Acetic Acid+ Methyl Acetate System, and in Five Binary Subsystems. *Fluid Phase Equilib.* **2006**, *247*, 96−101.
(102) Bonauguri, E.; Carpani, Z.; Dall'Orto, D. *Chim. Ind. Milan* **1956**, *38*, 768.
(103) Brown, I.; Ewald, A. Liquid-Vapour Equilibria. I. The Systems Carbon Tetrachloride-Cyclo-Hexane and Water-Acetic Acid. *Aust. J. Chem.* **1950**, *3*, 306−323.
(104) Chang, W.; Guan, G.; Li, X.; Yao, H. Isobaric Vapor- Liquid Equilibria for Water+ Acetic Acid+(n-Pentyl Acetate or Isopropyl Acetate). *J. Chem. Eng. Data* **2005**, *50*, 1129−1133.
(105) Freeman, J. R.; Wilson, G. M. *High Temperature Vapor-Liquid Equilibrium Measurements on Acetic Acid/Water Mixtures.* ; AIChE Symposium Series; Institute for Physical Property Data, 1985; Vol. *81*, p 14.
(106) Fu, H.; Chen, G.; Han, S. A Study on VLE of System Containing Associated Components(II)–VLE about Binary Systems of Acetic Acid-Water; Acetic Acid-2-Butanone; Acetic Acid-2-Pentanone; Acetic Acid-Propyl Acetate. *Huaxue Gongchengshi* **1986**, *6*, 56−61.
(107) Garwin, L.; Haddad, P. O. Dimethylaniline as an Aid in Acetic Acid−Water Separation. *Ind. Eng. Chem.* **1953**, *45*, 1558−1562.
(108) Gilmont, R.; Othmer, D. F. Composition of Vapors from Boiling Binary Solutions. *Ind. Eng. Chem.* **1944**, *36*, 1061−1064.
(109) González, B.; Domínguez, A.; Tojo, J. Dynamic Viscosities, Densities, and Speed of Sound and Derived Properties of the Binary Systems Acetic Acid with Water, Methanol, Ethanol, Ethyl Acetate and Methyl Acetate at T=(293.15, 298.15, and 303.15) K at Atmospheric Pressure. *J. Chem. Eng. Data* **2004**, *49*, 1590−1596.
(110) Granados, K.; Gracia-Fadrique, J.; Amigo, A.; Bravo, R. Refractive Index, Surface Tension, and Density of Aqueous Mixtures of Carboxylic Acids at 298.15 K. *J. Chem. Eng. Data* **2006**, *51*, 1356−1360.
(111) Keyes, D. B. Liquid-Vapor Composition Curves of Acetic Acid and Water at Subatmospheric Pressures. *Ind. Eng. Chem.* **1933**, *25*, 569.
(112) Lu, Y.; Cheng, Q.; Liu, M.; Han, Y.; Lou, X.; Lu, J. Calorimetric and Volumetric Studies of the Interactions of Butyramide in Aqueous Carboxylic Acid Solutions at 298.15 K. *Thermochim. Acta* **2002**, *386*, 103−110.
(113) Marek, J. Liquid-Vapor Equilibriums in Systems Containing an Associating Substance: III the System Water + Acetic Acid + Acetic Anhydride and the Corresponding Binary Systems at 400 Mm Mercury. *Chem. Listy* **1955**, *49*, 1756−1766.
(114) Marek, J. Effect of Association on Liquid-Vapor Equilibriums II. Correlation of Equilibriums of Binary Mixtures Containing Acetic Acid at Atmospheric Pressure. *Chem. Listy* **1955**, *49*, 957.
(115) Marek, J. Vapor-Liquid Equilibria in Mixtures Containing an Associating Substance. II. Binary Mixtures of Acetic Acid at Atmospheric Pressure. *Collect. Czech. Chem. Commun.* **1955**, *20*, 1490−1502.
(116) Navarro-Espinosa, I. R.; Cardona, C. A.; López, J. A. Experimental Measurements of Vapor−Liquid Equilibria at Low Pressure: Systems Containing Alcohols, Esters and Organic Acids. *Fluid Phase Equilib.* **2010**, *287*, 141−145.
(117) Othmer, D. F.; Silvis, S. J.; Spiel, A. Composition of Vapors from Boiling Binary Solutions: Pressure Equilibrium Still for Studying Water−Acetic Acid System. *Ind. Eng. Chem.* **1952**, *44*, 1864−1872.
(118) Pascal, P.; Dupuy, E.; Garnier, M. Study of Binary and Ternary Mixtures Found in the Manufacture of Synthetic Acetic Acid. *Bull. Soc. Chim. Fr.* **1921**, *29*, 9−21.

https://dx.doi.org/10.1021/acs.jced.9b01039
J. Chem. Eng. Data 2020, 65, 2405−2421

(119) Peng, Y.; Lu, X. Isobaric Vapor−Liquid Equilibria for Water+ Acetic Acid+ 1-Ethyl-3-Methylimidazolium Diethylphosphate at 101.32 KPa. *J. Chem. Eng. Data* **2014**, *59*, 250−256.
(120) Povarnin, G.; Markov, V. The System Acetic Acid - Water. *Zh Russ Fiz-Khim O-Va Chast Khim* **1924**, *55*, 381−382.
(121) Rivenc, G. Applications of Dynamic Ebulliometry: Isobaric Diagram of the System Water + Acetic Acid. *C. R. Congr. Natl. Soc. Savantes, Sect. Sci.* **1953**, *78E*, 459−462.
(122) Rivenc, G. Thermodynamic Study of Temperature-Vapor Composition and of Temperature- Liquid Composition Curves for Acetic Acid Water at 760mm. *Ind. Chim.* **1953**, *38*, 311−321.
(123) Vrevskii, M. S.; Mishchenko, K. P.; Muromtsev, B. A. The Dissociation of Acetic Acid Vapor and the Equilibrium between Its Aqueous Solutions and Their Vapors. *Zh Fiz Khim Russ Obshch* **1927**, *59*, 598.
(124) York, R., Jr.; Holmes, R. C. Vapor-Liquid Equilibria of the System Acetone-Acetic Acid-Water. *Ind. Eng. Chem.* **1942**, *34*, 345−350.
(125) Zhang, Y.; Zhang, J.; Fu, J. VLE OF ACETIC ACID-AQUA, ACETIC ACID-METHYL ACETATE, ACETIC ACID-AQUA-METHYL ACETATE. *Chem. Eng.* **1988**, *16*, 69.
(126) Zhong, X.; Huang, Y. Determination and Relating of VLE of Aceticacid-Methanoic Acid-Water System. *Chem. Eng.* **1983**, *5*, 64−72.
(127) Storn, R.; Price, K. Differential Evolution − A Simple and Efficient Heuristic for Global Optimization over Continuous Spaces. *J. Global Optim.* **1997**, *11*, 341−359.
(128) Jones, E.; Oliphant, E.; Peterson, P. *SciPy: Open Source Scientific Tools for Python*. 2001;Vol. *9*, p 10.
(129) Held, C.; Cameretti, L. F.; Sadowski, G. Modeling aqueous electrolyte solutions. *Fluid Phase Equilib.* **2008**, *270*, 87−96.
(130) Parisod, C. J.; Plattner, E. Vapor-Liquid Equilibriums of the Sodium Chloride-Water System in the Temperature Range 300-440 Degree.C. *J. Chem. Eng. Data* **1981**, *26*, 16−20.
(131) Bell, I. H.; Wronski, J.; Quoilin, S.; Lemort, V. Pure and Pseudo-Pure Fluid Thermophysical Property Evaluation and the Open-Source Thermophysical Property Library CoolProp. *Ind. Eng. Chem. Res.* **2014**, *53*, 2498−2508.

https://dx.doi.org/10.1021/acs.jced.9b01039
J. Chem. Eng. Data 2020, 65, 2405−2421